British Journal of Environment & Climate Change
2(2): 180-215, 2012

SCIENCEDOMAIN *international*
www.sciencedomain.org

Quantifying Uncertainties in the Modelled Estimates of Extreme Precipitation Events at Upper Thames River Basin

Tarana A. Solaiman[1*], Slobodan P. Simonovic[2] and Donald H. Burn[3]

[1]AMEC Americas Limited, Burlington, ON, Canada, L7N3G2.
[2]Department of Civil and Environmental Engineering, Western University, London, ON, Canada, N6A5B9.
[3]Department of Civil and Environmental Engineering, University of Waterloo, Waterloo, ON, Canada, N2L3G1.

Authors' contributions

This work was carried out in collaboration between the authors. The study was designed by all three authors. TAS performed the analysis, wrote the first draft and revised the manuscript. SPS and DHB provided input to the evaluation of results and reviewed the manuscript. All authors read and approved the final manuscript.

Research Article

Received 23rd April 2012
Accepted 17th July 2012
Online Ready 24th July 2012

ABSTRACT

Assessment of climate change impact on hydrology at watershed scale incorporates downscaling of global scale climatic variables into local scale hydrologic variables and evaluation of future hydrologic extremes. The climatological inputs obtained from several global climate models suffer the limitations due to incomplete knowledge arising from the inherent physical, chemical processes and the parameterization of the model structure. Downscaled output from a single AOGCM with a single emission scenario represents only one of all possible future climate realizations; averaging outputs from multiple AOGCMs might underestimate the extent of future changes in the intensity and frequency of climatological variables. These available methods, thus cannot be representative of the full extent of climate change. Present research, therefore addresses two major questions: (i) should climate research adopt equal weights from AOGCM outputs to generate future climate?; and (ii) what is the probability of the future extreme events to be more severe? This paper explores the methods available for quantifying uncertainties from the AOGCM outputs and provides an extensive investigation of the nonparametric kernel estimator

**Corresponding author: Email: tarana.solaiman@gmail.com;*

based on choice of bandwidths for investigating the severity of extreme precipitation events over the next century. The Sheather-Jones plug-in kernel estimate appears to be a major improvement over the parametric methods with known distribution. Results indicate increased probabilities for higher intensities and frequencies of events. The applied methodology is flexible and can be adapted to any uncertainty estimation studies with unknown densities. The presented research is expected to broaden our existing knowledge on the nature of the extreme precipitation events and the propagation and quantification of uncertainties arising from the global climate models and emission scenarios.

Keywords: Climate change; water resources; uncertainty estimation; kernel density; global climate models.

1. INTRODUCTION

Current practice of hydrologic research and modeling is largely dependent on climatological inputs with the increased interest in climate change impact assessment studies in water resources. Assessment of climate change impacts on hydrology incorporates downscaling of global scale climatic variables into local scale hydrologic variables and computations of risk of hydrologic extremes in future for water resources planning and management. Recent studies related to Canadian climate have indicated 12% increase of precipitation in southern Canada during the twentieth century (Zhang et al., 2000; Vincent and Mekis, 2006). Climate modeling studies involving anthropogenic increase in the concentration of greenhouse gases have also suggested an increase in the frequency and intensity of climatic extremes in a warmer world (Cubasch et al., 2001). However, most efforts are focused on studying the changes of means, although extremes usually have the greatest and most direct impact on our everyday lives, community and environment. Analysis of intense precipitation over Canadian climate have shown (i) largest relative increase and a shift in summer time heavy precipitation more towards spring during daytime over inland regions, particularly in Ontario and Southern Quebec (Mailhot et al., 2010; Mailhot et al., 2011).

Coupled Atmosphere-Ocean Global Climate Models (AOGCMs) provide a numerical representation of the climate system based on the physical, chemical and biological properties of their components and feedback interactions between them (IPCC, 2007). They are currently the most reliable tools available for obtaining the physics and chemistry of the atmosphere and oceans and to derive projections of meteorological variables (temperature, precipitation, wind speed, solar radiation, humidity, pressure, etc). They are based on various assumptions about the effects of the concentration of greenhouse gases in the atmosphere coupled with projections of CO_2 emission rates (Smith et al., 2009).

There is a high level of confidence that AOGCMs are able to capture large scale circulation patterns and correctly model smoothly varying fields such as surface pressure, especially at continental or larger scales. However, it is extremely unlikely that these models properly reproduce highly variable fields, such as precipitation (Hughes and Guttorp, 1994), on a regional scale, let alone, for small to medium watershed. Although confidence has increased in the ability of AOGCMs to simulate extreme events, such as hot and cold spells, the frequency and the amount of precipitation during intense events are still underestimated.

Climate change impact studies derived from AOGCM outputs are associated with uncertainties due to "incomplete" knowledge originating from insufficient information or understanding of biophysical processes or a lack of analytical resources. Examples include simplification of complex processes involved in atmospheric and oceanographic transfers, limited assumptions about climatic processes, limited spatial and temporal resolution resulting in a disagreement between AOGCMs over regional climate change, etc. Uncertainties also emerge due to "unknowable" knowledge arising from the inherent complexity of the Earth system and from our inability to forecast future socio-economic and human behavior in a deterministic manner (New and Hulme, 2000; Allan and Ingram, 2002; Proudhomme et al., 2003; Wilby and Harris, 2006; Stainforth et al., 2007; IPCC, 2007; Buytaert et al., 2009). Selection of the most appropriate AOGCM for realization of future climate depends on user's ability to assess model's strengths and weakness and is recognized as one of the major sources of uncertainty (Wilby and Harris, 2006; Ghosh and Mujumdar, 2007; Tebaldi and Smith, 2010). Utilization of a single AOGCM represents one of all possible realizations and cannot be representative of the future. So, for a comprehensive assessment of the future changes, it is important to use collective information by utilizing all available models, synthesizing the projections and uncertainties in a probabilistic manner. In recent years, quantifying uncertainties from AOGCM choice and scenario selections used for impact assessments has been identified as a critical climate change and adaptation research. Multi-model ensemble systems as well as multi-member ensembles are two such methods for investigating the impact of model structures on future change in extreme precipitation/rainfall events (Mailhot et al., 2007).

The earliest work, to our knowledge, considering a multi-model ensemble approach was of Raisanen and Palmer (2001) who treated the ensemble members as equally probable realizations and determined probabilities of climate change by computing the fraction of ensemble members in which the differential properties of models, such as bias and rate of convergence was disregarded. Giorgi and Mearns (2003) confronted their approach by introducing "Reliability Ensemble Averaging (REA)" technique considering reliability based likelihood of realization by models to calculate the probability of regional temperature and precipitation change and found it more flexible in assessment of risk and cost in regional climate change studies. Tebaldi et al. (2004, 2005) used Bayesian statistics to estimate a distribution of future climates from the combination of past observed and the corresponding AOGCM simulated climates motivated by the assumptions that an AOGCM ensemble is a "sample of the full potential climate model space compatible with the observed climate using probability distributions (PDFs)" at a regional scale.

Recently, Smith et al. (2009) extended their work by introducing univariate approach to consider one region at a time. They are still using a multivariate approach, including cross validation, to confirm the resemblance of the Bayesian predictive distributions. Other literature on Bayesian methods in multimodel ensembles includes work from Allan et al. (2005), Benestad (2004), Stone and Allan (2005) and Jackson et al. (2004).

Wilby and Harris (2006) developed a probabilistic framework to combine information from four AOGCMs, two greenhouse scenarios where the AOGCMs were weighted to an index of reliability for downscaled effective rainfall. A Monte Carlo approach was followed to explore components of uncertainty affecting projections for the river Thames for 2080s. The resulting cumulative distribution functions appeared to be most sensitive to uncertainty in: (i) the selection of climate change scenarios; and (ii) downscaling of different AOGCMs.

In order to estimate uncertainties at smaller spatial scales, output from climate models should be scaled down at suitable level. Statistical and dynamic downscaling are two commonly used techniques for the development of climate scenarios depending on their accuracy for different seasons, regions, time periods and the variables of interest. However, studies have indicated that the task of downscaling sometimes becomes challenging due to the absence of proper station measurements. Gridded databases, such as the National Center for Environmental Prediction – National Center for Atmospheric Research (NCEP-NCAR) Global Reanalysis – NNGR (Kalnay et al., 1996) and North American Regional Reanalysis – NARR (Mesinger et al., 2006) can be viable alternatives to alleviate these limitations of missing data and spatial bias resulting from uneven and unrepresentative spatial modelling (Robeson and Ensor, 2006; Ensor and Robeson, 2008). The reanalysis data are advantageous in impact studies because they are based on the AOGCMs with a fixed dynamic core, physical parameterizations and data assimilation system (Castro et al., 2007).

Reanalysis databases are also gaining use in uncertainty assessment studies. Ghosh and Mujumdar (2007) used NNGR to develop a methodology to assess AOGCM uncertainty due to different AOGCMs by considering different probability density function for each time step. They used the information on uncertainty in examining future drought scenarios in a nonparametric manner. Samples of drought indicators were generated with results from downscaled precipitation using statistical regression approach from available AOGCMs and scenarios. The severity of droughts was presented in a nonparametric kernel estimation and orthonormal approach.

In many applications, the NNGR resolution (250 km × 250 km) is not satisfactory, especially in regions with complex topography (Choi et al., 2009; Tolika et al., 2006; Rusticucci and Kousky, 2002; Haberlandt and Kite, 1998; Castro et al., 2007).

The NARR dataset (Mesinger et al., 2006) is a major improvement upon the global reanalysis datasets in both resolution and accuracy. Literature related to inter-comparison between the global and regional datasets (Nigam and Ruiz-Barradas, 2006; Woo and Thorne, 2006; Castro et al., 2007; Choi et al., 2007, 2009) shows better agreement of NARR data. More recently, Solaiman and Simonovic (2010) made a rigorous assessment of the NARR and NNGR database for application in the Upper Thames river basin (Ontario, Canada) for hydrological modeling and/or climate change impact studies.

It is important to note that work dealing with the implications of uncertainties in estimating the severity of extreme precipitation events is not available yet extensively in the literature. In this paper, an attempt has been made to compare the predictions of precipitation change on a watershed scale by two very different methods: (i) downscaling approach using a principal component analysis integrated nonparametric K-nearest neighbor weather generator; and (ii) Bayesian reliability ensemble method (BA-REA) as described by Tebaldi et al. (2004, 2005). Next, a classification scheme for investigating severity level of extreme precipitation indices is addressed. Finally, the nonparametric data driven kernel density estimation methods are investigated to quantify uncertainties associated with AOGCM and scenario outputs.

2. CASE STUDY

2.1 Study Area

The Upper Thames River (UTR) basin (Fig. 1) (42º35'24''N, 81º8'24''W), situated in south-western Ontario, Canada, is a 3,500 km^2 area nested between the Great Lakes Huron and Erie. The population of the basin is 450,000 (2006) of which 350,000 are the residents of the City of London. The Thames River is about 273 km long with an average annual discharge of 39.3 m^3/s. Thames River basin consists of two major tributaries of the river Thames: the North branch (1,750 km^2), flowing southward through Mitchell, St. Marys, and eventually into London where it meets the South branch; and the South branch (1,360 km^2) flowing through Woodstock, Ingersoll and east London. The basin receives about 1,000 mm of annual precipitation, 60% of which is lost through evaporation and/or evapotranspiration, stored in ponds and wetlands, or recharged as groundwater (Prodanovic and Simonovic, 2006).

2.2 Database

Daily precipitation and temperature are the most important atmospheric forcing parameters required for any hydrologic impact study for a larger river basin (Salathe Jr., 2003). However, climate models do not resolve important mesoscale and surface features that control precipitation in an area. The choice of appropriate predictors or characteristics from the large-scale atmospheric circulation is one of the most important steps in downscaling. Rainfall can be related to air mass transport and thus related to atmospheric circulation, which is a consequence of pressure differences and anomalies (Bardossy, 1997). Mean sea level pressure is the basis of derived variables such as surface vorticity, airflow strength, meridional and zonal flow components and divergence (Wilby and Wigley, 2000). Specific humidity is reported to have significance to AOGCM precipitation schemes (Hennessy et al., 1997). Considering all the above factors, predictor variables mentioned in Table 1 are initially chosen to generate precipitation in this study. Daily observed precipitation (precip), maximum and minimum temperature (Tmax and Tmin) data from 22 stations covering the UTR basin for the period of 1979-2005 is collected from the Environment Canada [http://www.climate.weatheroffice.gc.ca/climateData/canada_e.html]. The rest of the atmospheric variables are collected from NARR reanalysis dataset for a period of 1979 – 2005. Precipitation values less than 0.5 mm day^{-1} is considered zero as suggested by Reid et al. (2001) and Choi et al. (2007). NARR data for this study has been made available through the Data Access Integration of the Canadian Climate Change Scenarios Network of Environment Canada.

Table 1. Definition of predictor variables

Predictors	Abbreviations
Precipitation (mm/day)	Precip
Maximum temperature (ºC)	Tmax
Minimum temperature (ºC)	Tmin
Mean sea level pressure (Pa)	MSL
Specific humidity (Kg/ Kg)	SPFH
Zonal (eastward) wind velocity component (m/s) at 10 m	UGRD
Meridional (northward) wind velocity component (m/s) at 10 m	VGRD

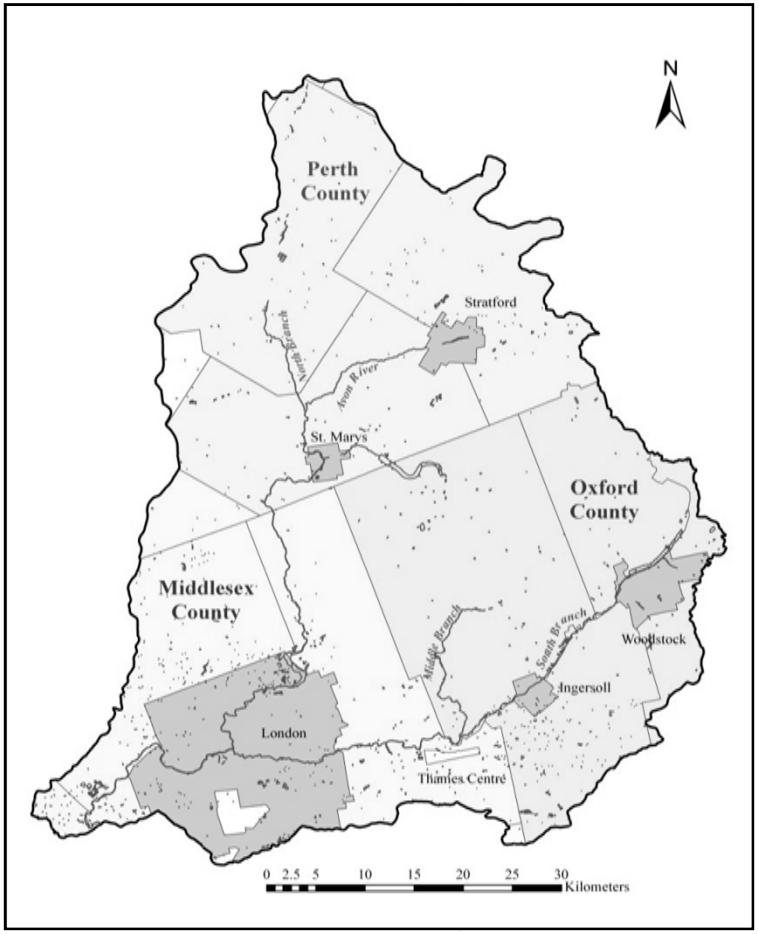

Fig. 1. The upper Thames river basin

Future climate scenarios are generated using predictor variables (Table 1) and six different AOGCM models, each with 2 to 3 emission scenarios (balanced across all energy sources (A1B), the high end (A2), and the medium, more ecologically friendly (B1)) from the Intergovernmental Panel on Climate Change Special Report in Emission Scenarios (IPCC SRES) for three future time slices 2020s, 2050s and 2080s (Table 2). Both NARR and the AOGCM datasets are processed to conform to the station's grid points.

Table 2. List of AOGCM models and emission scenarios used

GCM models	Sponsors, Country	SRES scenarios	Atmospheric resolution	
			Lat	Long
CGCM3T47, 2005	Canadian Centre for Climate Modelling and Analysis, Canada	A1B, A2, B1	3.75º	3.75º
CGCM3T63, 2005		A1B, A2, B1	2.81º	2.81º
CSIROMK3.5, 2001	Commonwealth Scientific and Industrial Research Organization (CISRO) Atmospheric Research, Australia	A2, B1	1.875º	1.875º
GISSAOM, 2004	National Aeronautics and Space Administration (NASA)/ Goddard Institute for Space Studies (GISS), USA	A1B, B1	3º	4º
MIROC3.2HIRES, 2004	Centre for Climate System Research (University of Tokyo),	A1B, B1	1.125º	1.125º
MIROC3.2MEDRES, 2004	National Institute for Environmental Studies, and Frontier Research Centre for Global Change (JAMSTEC), Japan	A1B, A2, B1	2.8º	2.8º

3. METHODOLOGY

Two approaches based on fundamentally different assumptions are applied to estimate uncertainty in climate model projections of future precipitation under different forcing scenarios. First, a methodology is developed by combining statistical downscaling using PCA based weather generator approach and nonparametric kernel density estimation technique. Next, a Bayesian statistics approach is applied to estimate a distribution of future climates, from the combination of past observed and corresponding AOGCM-simulated data.

3.1 Statistical Downscaling Combined with Nonparametric Method

3.1.1 Weather generator based downscaling

Weather generators are tools for generating sequences of weather variables. They can also be regarded as complex number generators, the output of which resembles daily weather data at a particular location. The parameters of the weather generators are conditioned upon a large scale state, or the relationships between daily weather generator parameters and climatic averages. The early work using weather generators as a downscaling tool in climate

change studies can be found in Hughes (1993), Hughes and Guttorp (1994), Hughes et al. (1999) and Wilks and Wilby (1999). Examples of weather generators (WG's) which have been successfully employed in climate change studies are LARS-WG (Semenov and Barrow, 1997), K-NN (Yates et al., 2003; Sharif and Burn, 2006) and EARWIG (Kilsby et al., 2007).

Considerable research effort has been undertaken to statistically model the precipitation extremes, with much evidence of their heavy-tailed distribution (Koutsoyiannis, 2004). Weather generators are made to consistently model the precipitation extremes with heavy-tailed distribution. But the use of weather generators in improving simulation of precipitation extremes is limited. Furrer and Katz (2008) proposed several possible advanced statistical approaches for improving the treatment of extremes within a parametric Generalized Linear Modeling (GLM) based stochastic weather generator framework. They found a substantial improvement with a hybrid technique with a gamma distribution for low to moderate intensities and a generalized Pareto distribution for high intensities. Sharif and Burn [2006] used nonparametric K-nearest neighbour weather generator model for simulating extreme precipitation events and found encouraging results in simulating extreme dry and wet spells.

The initial version of the weather generator, used in this study was developed based on a K-NN resampling strategy (Yates et al., 2003; Sharif and Burn, 2006). The major drawback of the K-NN weather generator developed by Yates et al. (2003) was the same observed max-min range as that of the synthetic dataset. Sharif and Burn (2006) improved this algorithm by adding a perturbation process that can calculate alternative extremes for the dataset. The tool underwent several minor modifications (Prodanovic and Simonovic, 2006; Eum et al., 2009). The present version incorporates principal component analysis to reduce the multicollinearity of the predictor variables. A detailed description of the weather generator used for this study can be found in Solaiman et al. (2011).

3.1.2 Kernel method for estimating uncertainties

A practical approach to deal with AOGCM and scenario uncertainties initiating from inadequate information and incomplete knowledge should: (1) be robust with respect to model choice; (2) be statistically consistent in a uniform application across different area scales such as global, regional or local/watershed scales; (3) be flexible enough to deal with the variety of data; (4) obtain the maximum information from the sample; and (5) lead to consistent results. Most parametric methods do not meet all these requirements.

Probability distribution functions estimated by any nonparametric method, such as kernel density estimator without prior assumptions can be suitable to quantify AOGCM and scenario uncertainties. Kernel density estimation method has been widely used as a viable and flexible alternative to parametric methods in hydrology (Sharma et al., 1997; Lall, 1995), flood frequency analysis (Lall et al., 1993; Adamowski, 1985) and precipitation resampling (Lall et al., 1996) for estimating probability density function.

A kernel density estimate is formed through the convolution of kernels or weight functions centered at the empirical frequency distribution of the data. Given a sample of $\{X_1, \ldots\ldots, X_i, \ldots\ldots, X_n\}$ with a sample size n and density f, the Parzen-Rosenbalt kernel density estimate $\hat{f}_k(x)$ at any point x is given by:

$$\hat{f}_k(x) = \frac{1}{nh}\sum_{j=1}^{n} K\left(\frac{x-X_j}{h}\right) \quad (1)$$

Where $t = \left(\frac{x - X_j}{h}\right)$ and $k(t)$ is a weight or kernel function required to satisfy criteria such as symmetry, finite variance, and integrates to unity. Successful application of any kernel density estimation depends more on the choice of the smoothing parameter or bandwidth (h) and the type of kernel function $K(.)$, to a lesser extent.

Bandwidth for kernel estimation may be evaluated by minimizing the deviation of the estimated PDF from the actual one. Assuming normal distribution for the bandwidth estimation, the optimal bandwidth for a normal kernel can be given by (Polansky and Baker, 2000):

$$h_n = (1.587)\hat{\sigma} n^{-\frac{1}{3}} \quad (2)$$

Where $\hat{\sigma}$ is the sample standard deviation measured by Silverman (1986):

$$\hat{\sigma} = min\left\{S, {}^{IQR}/_{1.349}\right\} \quad (3)$$

Where *S* is the sample standard deviation and *IQR* is the interquartile range.

This methodology is applied to derive PDF of mean monthly precipitation at different time steps.

3.1.3 Data preprocessing and experimental setup

A schematic of estimating the PDFs combining uncertainties using downscaling technique is presented in Fig. 2. For this study, daily input variables from NARR as indicated in Table 1 are collected at the nearest grid points and spatially interpolated to the stations surrounding the Upper Thames River basin.

For selection of appropriate conditioning variables, several combinations of predictors from Table 1 are used to generate synthetic versions of the historic dataset. A multi-objective Compromise Programming tool is then used to find an optimal set of predictors. Assessment of trade-offs between different combinations of variables (considered as alternatives) is done according to four variability measures (considered as criteria): mean, standard deviation, maximum and minimum values for each month. The rank of each combination is measured by the Compromise Programming distance metric which is calculated as the distance from the ideal solution for each alternative. Table 3 presents the ranks obtained for each combination of predictors. It is clearly seen that a combination of all seven predictors is the closest to the ideal solution in most months and hence, is selected for further analysis.

Next, the monthly information from each of the AOGCM emission scenarios (Table 2) is collected for four time slices: 1961-1990, 2011-2040, 2041-2070 and 2071-2100. Climate variables from nearest grid points have been interpolated to provide a dataset for each of the stations of interest in the same way as the NARRs. In order to generate future climate data, the difference between the base climate (1961-1990) and the AOGCM outputs (2041-2070 or 2050s) are computed for all predictors. These monthly change fields are then used to modify the historic dataset collected for each station to create future dataset.

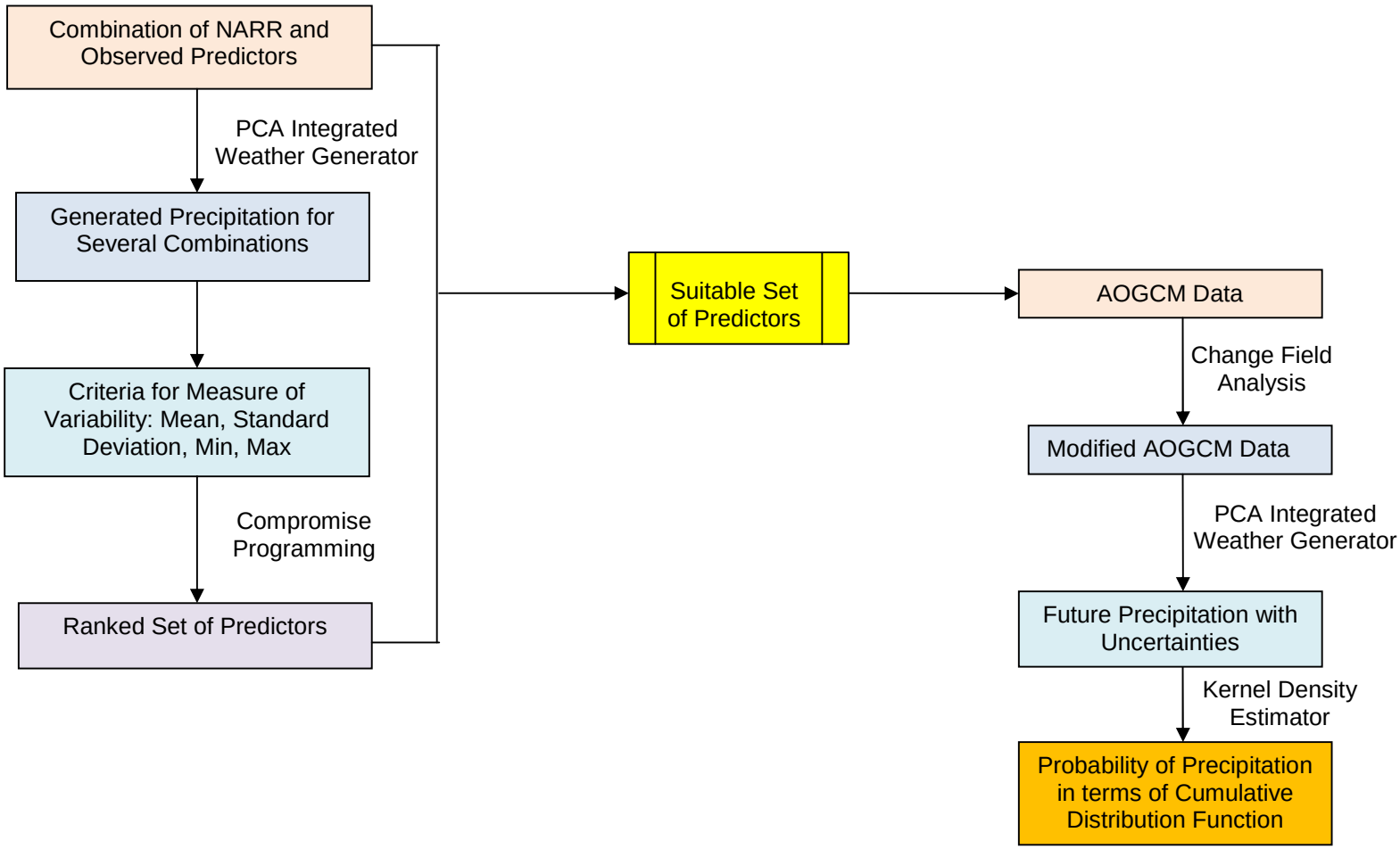

Fig. 2. Flow chart of uncertainty estimation using statistical downscaling

Table 3. Rank table of different combinations of predictors

Cases	Jan	Feb	Mar	Apr	May	Jun	Jul	Aug	Sep	Oct	Nov	Dec
P, Tmax, Tmin, PRMSL	7	6	5	6	3	1	1	5	7	4	6	1
P, Tmax, Tmin, PRMSL, SPFH	4	1	7	5	4	2	7	7	6	1	3	7
P, Tmax, Tmin, PRMSL, SPFH, UGRD, VGRD	**5**	**2**	**2**	**4**	**2**	**4**	**3**	**3**	**1**	**6**	**4**	**2**
P,Tmax,Tmin,PRMSL,UGRD,VGRD	6	4	1	7	7	5	2	1	4	2	5	6
P, Tmax, Tmin, SPFH	3	7	4	1	5	3	6	2	5	3	7	4
P, Tmax, Tmin, SPFH, UGRD, VGRD	2	3	6	3	1	7	5	6	3	5	2	5
P, Tmax, Tmin, UGRD, VGRD	1	5	3	2	6	6	4	4	2	7	1	3

** P: Precipitation, Tmax: Maximum temperature, Tmin: Minimum temperature, PRMSL: Mean sea level pressure, SPFH: Specific humidity, UGRD: Eastward wind component , VGRD: Northward wind component*

In order to reduce multi-dimensionality and collinearity associated with the large number of input variables, principal component analysis is integrated with the weather generator. The process requires selection of appropriate principal components (PCs) that will adequately represent most information in the original dataset. It is found that the first PC is able to explain over 80% of the variations associated with the inputs. Hence, only first PC is considered for the weather generator.

The daily future data downscaled using WG-PCA, are averaged to monthly value to draw PDF for the comparison with the BA-REA approach. The average monthly total values for winter (DJF) and summer (JJA) for each scenario are considered. Values from each AOGCM for any specific year are considered as an independent set of realization and are used to draw PDFs.

3.2 The Bayesian Reliability Ensemble Average Method (Tebaldi et al. Approach)

The methodology developed by Tebaldi et al. (2004, 2005) consists of a formal Bayesian implementation and extension of the reliability ensemble averaging (REA) approach of Giorgi and Mearns (2002, 2003) to combine data from observations and a multi-model ensemble of AOGCMs to compute PDFs of future temperature and precipitation change over large regions under different forcing scenarios. The reliability of any AOGCM is measured by two criteria to form the shape of the posterior distribution as a consequence of assumptions formulated in the statistical model: mean bias of present climate and rate of convergence of the future climate models to weighted ensemble mean. In the following two sections major components, data processing and experimental set up of the model are presented.

3.2.1 Model parameters

In the Bayesian framework, all parameters such as the present and future variable responses from any AOGCM response are considered as random variables. It constitutes mainly of three components: the prior, likelihood and posterior. In cases with lack of previous information, this model considers un-informative prior allowing a wide range of possible values. The second component is the distribution (likelihood) of the data which is a function of random parameters. In their study, Tebaldi et al. (2004, 2005) assumed a symmetric distribution centered on the 'true' value of variable as a measure of the ability of any AOGCM for a given set of forcing. The assumption of a symmetric distribution (normal distribution) around the 'true' value of precipitation for the suite of multi-model responses has been implicitly supported by CMIP studies (Meehl et al., 2000). However, the assumption of normality may be appropriate in their study of large regions, but it is highly unlikely that the distribution of variable precipitation can be approximated by a normal curve for a small and/or single region.

The prior and likelihood is combined through Bayes' theorem into the joint posterior distribution for the random variables in the model. The empirical estimate of the posterior distribution is obtained through Markov Chain Monte Carlo (MCMC) simulation. The description of the algorithm can be found in detail in Tebaldi et al. (2004).

For univariate approach, Tebaldi et al. (2004; 2005) divided the entire globe into 22 regions but each of the 22 regions was treated as a separate variable; each scenario was also treated separately, which ignores scenario uncertainties. For this study, area averaged precipitation response from all 15 AOGCMs and scenarios, averaged for the London station

is considered to compare with the PDFs generated by the methodology presented in Section 3.1.

3.2.2 Data and model setup

To generate PDF of precipitation affected by the climate change, simulated present (1961-1990) and future (2041-2070) precipitation (X_i, Y_i) are considered for winter (December-January-February) and summer (June-July-August) seasons. The outputs from 15 different set of experiments from 6 AOGCMs for the two time slices are extracted for the 22 stations and averaged for the London station using nearest neighbor approach. The natural variability is expressed as the inverse of the variance of observed precipitation for 1961-1990 (X_0). It is calculated as the interannual variance on the basis of the observed record (X_0). The computer codes used in this study can be downloaded from National Centre for Atmospheric Research website (*http://www.image.ucar.edu/~nychka/REA/*).

3.3 Indexing Extreme Precipitation Events

Simulation of extreme precipitation is dependent on resolution, parametrization and the selected thresholds. Sun et al. [2006] found that most AOGCM models tend to produce light precipitation (<10mm day^{-1}) more often than observed, too few heavy precipitation events and much less precipitation during heavy events (>10 mm day^{-1}) (Randall et al., 2007). The situation gets worse in the absence of any extreme precipitation indices. In the IPCC (2007), several indices explaining extreme temperature and precipitation are proposed but most literature reports investigations of percent change in the occurrences of such indices without any acceptable definition of their severity level.

Three precipitation indices have been used for comparing the performance of the AOGCMs in generating extreme precipitation amounts. These indices describe precipitation frequency, intensity and extremes. The highest 5 day precipitation, number of very wet days and the number of heavy precipitation days express extreme features of precipitation. For very wet days, the 95th percentile reference value has been obtained from all non-zero total precipitation events for the base climate. Heavy precipitation days are those days that experience more than 10 mm of precipitation.

For Canada, due to large variation of precipitation intensities in various regions, a fixed threshold may not be good to assess the severity level (Vincent and Mekis, 2006). So in this study, an attempt has been made to classify the severity level of these indices based on percentile values. The percentile method has several advantages. It is simple and computationally inexpensive. It is completely data driven and does not follow any specific distribution, so can be used at any location with different precipitation patterns. Table 4 presents the classification scheme used for summer and winter season. Like the widely known drought indicators, the precipitation events are named as near normal, mild, moderate, severe, and extreme as compared to the baseline climate (1961-1990). They can be easily used to assess the impact of climate change on extreme precipitation events.

Table 4. Classification extreme precipitation indices based on percentile method

Serial	Description
1	<= 25th percentile of 1961-1990 observed precipitation
2	25th – 50th percentile of 1961-1990 observed precipitation
3	50th –75th percentile of 1961-1990 observed precipitation
4	75th – 95th percentile of 1961-1990 observed precipitation
5	>95th percentile of 1961-1990 observed precipitation

3.4 Nonparametric Methods of Quantifying Uncertainties of Extreme Precipitation Events

Nonparametric estimators are erroneously considered to be less accurate with small sample sizes. However, this may not always be true (Lall et al., 1993). With increase in sample size, the choice of estimator selection (parametric or nonparametric) can only be identified well. For assessing AOGCM and scenario uncertainties of future droughts, Ghosh and Mujumdar (2007) applied two nonparametric methods: (i) the kernel density estimation method based on Silverman (1986), and (ii) the Orthonormal method of Efromovich (1999). In this paper, the application of normal kernel estimator is extended with the commonly used bandwidth selection methods for estimating densities and address model choice and scenario choice uncertainties.

3.4.1 Definition

The kernel density estimation described in section 3.1.4 (equation 1) is based on the method of assuming normal distribution function for unknown PDFs. The quantification of uncertainties using kernel density estimate is further extended based on the choice of smoothing parameter or bandwidth. A change in bandwidth can dramatically change the shape of the kernel estimate (Efromovich, 1999).

3.4.2 Methods for bandwidth selection

Jones et al. (1996) classified several data driven estimation methods as first generation (methods proposed before 1990) and second generation (methods proposed after 1990). The most basic method is the 'rule of thumb' used by Silverman (1986). The idea involves replacing unknown part of h_{AMISE}, by an estimated value based on a parametric family such as a normal distribution, $N(0,\sigma^2)$. However, this method provided oversmoothed function (Terrell and Scott, 1985; Terrell, 1990) and proved to be unrealistic in many applications. The application of rule of thumb has been more successful for near normal densities.

For kernel density estimations, the integrated squared error loss functions are evaluated for selecting suitable bandwidths. The idea of 'least squared cross validation', first used by Bowman (1984) and Rudemo (1982) incorporates integrated squared error (ISE) as

$$ISE(h) = \int \left(\widehat{f_h}(x) - f(x)\right)^2 = \int \hat{f}_h(x)^2 - 2\int \hat{f}_h(x)\, f(x) + \int f(x)^2 \qquad (4)$$

The term $\int \hat{f}_h(x)^2$ depends on the density estimate and can be evaluated numerically. The third term $\int f(x)^2$ does not depend on *h* and can be ignored. The remaining term $\int \hat{f}_h(x) f(x)$ can be estimated by $-2n^{-1} \sum_{i=1}^{n} \hat{f}_h(X_i)$, where $\hat{f}_i$ is the leave out kernel density estimator defined by Hall and Marron (1991). The use of LCV method with kernel density estimation has been unsatisfactory due to their sensitiveness around the tailed data where the kernel estimates have shown poor performances. They are more suitable for local regression and likelihood models (Loader, 1999).

The plug in methods are based on the bias of an estimate $\hat{f}$, written as a function of the unknown f and usually approximated through Taylor series expansions. A pilot estimate of f is then plugged in to derive the estimate of the bias and hence the estimate of mean integrated squared error. The optimal h minimizes this estimated measure of fit. The plug-in method produces a bandwidth with relative rate of convergence of order $n^{-1/2}$. Detailed description of plug-in kernel method can be found in Sheather and Jones (1991) and Jones et al. (1996)

4. RESULTS AND DISCUSSION

The comparison of performance for different methods presented in this paper is shown for London station. First, the performance of weather generator in producing the present day climate is evaluated. Then, a comparative assessment of uncertainties by the downscaled data with kernel estimator and the Bayesian based reliable ensemble average (BA-REA) techniques is shown. Next, the indices for estimating the severity of extreme precipitation events are developed. Finally, the probabilities of extreme precipitation events are assessed with associated AOGCM and scenario uncertainties.

4.1 Model Performance Evaluation in Estimating Uncertainties

Prior to discussing the climate change results, it is important to provide an overall view of the model performance in reproducing present climate. To compute the PDF of the transient climate response (a) the BA-REA method and (b) the WG-PCA combined with kernel estimation method are applied and the results are compared using density curves.

4.1.1 Downscaling model performance

This study uses 22 stations for the period of 1979-2005 (N=27 years) to simulate precipitation scenarios using seven meteorological variables. Employing the temporal window of 14 days (w=14) and 27 years of historic data (N=27), 404 days are considered as potential neighbors *(L=(w+1) x N-1=404)* for each variable. 12 different runs, each comprising of 27 years of daily precipitation are generated. Errors in the estimates of mean and variance of generated precipitation are evaluated using statistical hypothesis test at 95% confidence level.

The performance of WG in representing the present climate is tested using nonparametric Wilcoxon-rank test and Levene's test. Table 5 presents statistical significance test results (*p* values) in the estimate of daily precipitation for summer (JJA) and winter (DJF) for 1979-2005 in London. The *p* values at 95% confidence level for all runs are above the threshold (*0.05*) which clearly indicates that there is no evidence of different means between the observed and generated precipitations. The results of the Levene's test for the equality of variances of observed and simulated precipitation at 95% confidence level are presented in

Table 5. The *p* values appear above 0.05 thresholds, indicating equal variability of the simulated precipitation with the observed precipitation. So, the observed and the simulated precipitation can be assumed to have equal variances.

Table 5. Test results (*p* values) of the Wilcoxon Rank test and Levene's test for the difference of means and equality of variances of historical observed and simulated precipitation at 95% confidence level

Runs	*Wilcoxon Rank test*		*Levene's test*	
	Summer	Winter	Summer	Winter
1	0.46	0.48	0.61	0.55
2	0.76	0.61	0.72	0.58
3	0.64	0.67	0.56	0.99
4	0.93	0.37	0.98	0.18
5	0.60	0.98	0.87	0.59
6	0.59	0.53	0.96	0.99
7	0.91	0.95	0.64	0.20
8	0.91	0.95	0.64	0.20
9	0.76	0.67	0.98	0.84
10	0.48	0.63	0.91	0.19
11	0.77	0.80	0.41	0.66
12	0.76	0.29	0.76	0.30

Frequency distributions of wet-spell lengths for winter and summer months are plotted in Fig. 3. A comparison of observed and simulated values for wet-spell lengths shows very close agreement between the frequency distributions. The frequency of wet-spell lengths in the simulated data for summer is almost identical to the observed values, except for the one day lengths where the simulated data show slight overestimation. Same is the case for the winter months. The performance of weather generator in reproducing wet-spell lengths is very good.

Using the synthetic data set created from the change factors from several AOGCMs, 324 years of data set is generated for each case. The generated precipitation for the future periods is then reduced to mean seasonal values to compare the results with the BA-REA method. Mean precipitation obtained from each AOGCM and scenario is then assumed to be an independent realization of future. Using this concept, climate density curves are generated combining the information from all AOGCMs for 2050s, the results of which are presented in section 4.1.3.

4.1.2 BA-REA model performance

The performance of the model can be assessed by model bias and convergence. Table 6 presents the values of the bias from 6 different AOGCMs. Bias is calculated as the difference between each AOGCM's response to the present climate and the present climate as generated by the BA-REA model. The base climate values generated from different AOGCMs are equal irrespective of all future scenarios (Such as A1B, B1 or A2). Fig. 4 presents posterior distributions of precipitation change $\Delta P = \nu - \mu$ for London during winter and summer seasons, where ν and μ represents the true present and future precipitations, respectively. For reference, the response of 15 models and scenarios' individual

responses $Y_i - X_i$, for *i=1, 2, …., 15* are plotted along the x axis (dots) together with REA estimate of mean change (triangles). A measure of convergence can be assessed from the relative position of the individual responses. The relative position is used in identification of the outlier models and models that reinforce each other.

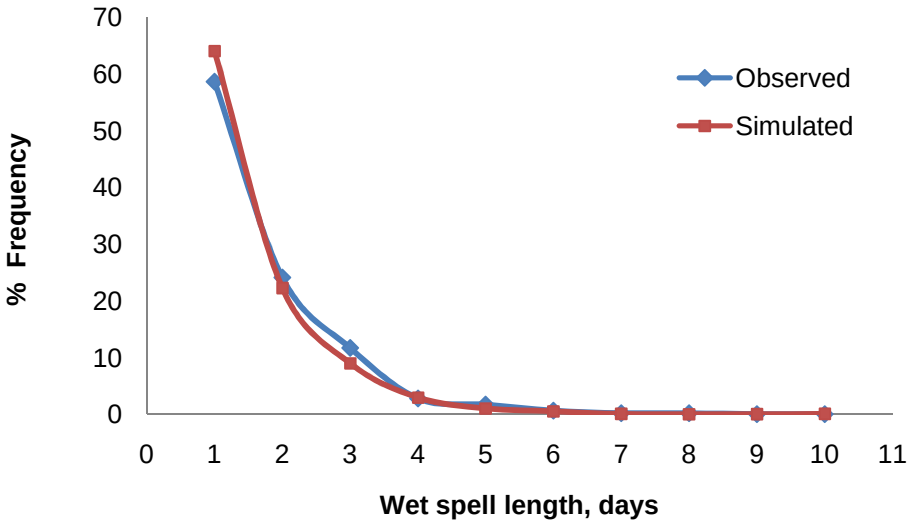

(a)

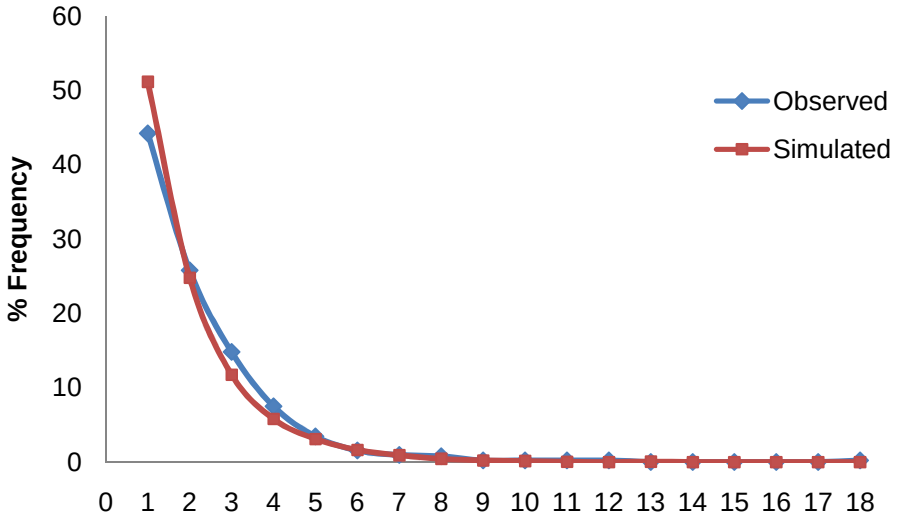

(b)

Fig. 3. Frequency plots of wet spell lengths for summer (a) and winter (b)

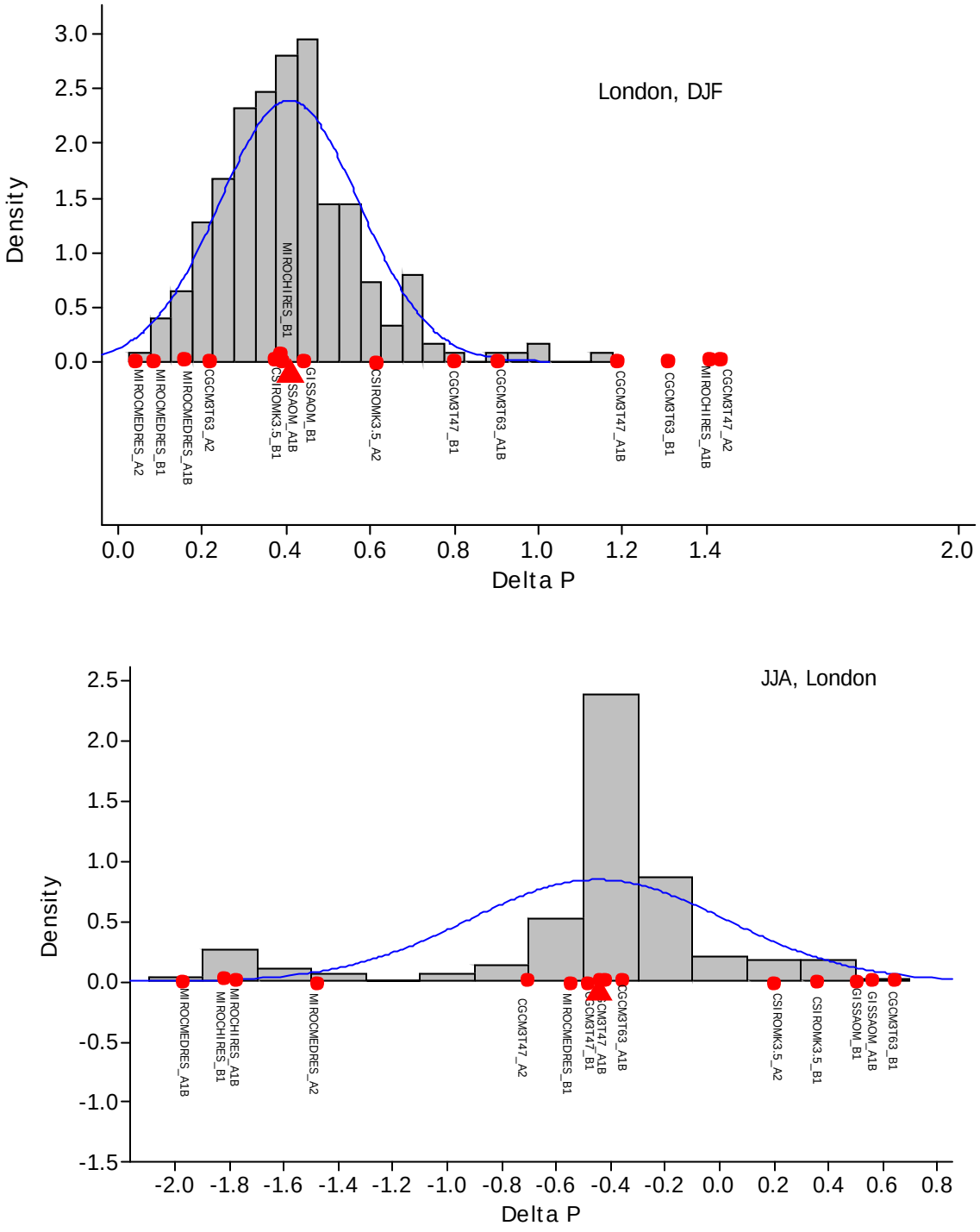

Fig. 4. Posterior distributions of Delta P= ν – μ explaining the differences between future and base climate change in London for winter (DJF) and summer (JJA) season.

The comparison of densities in Fig. 4 and bias measure in Table 6 identify the models that provide higher biases (Table 6) and act as outliers (Fig. 4). Biases are calculated as the deviation of the single AOGCM's response Xi, from the mean of the posterior distribution μ derived by the analysis. Models with smaller biases receive larger weights. The cases that respect both criteria are the ones where the probability density is concentrated. Solid line in Fig. 4 shows the fitted curve. The points along the base of the densities mark predicted precipitation change from the 15 AOGCM scenarios for 2050s. The triangle indicates the REA estimate of mean change. Next, the relative weighting of different AOGCM scenarios are calculated using the posterior mean for each λ_i, and standardized to percentages for both seasons. The results are presented in Table 7. The values are computed as $\frac{100 \cdot \lambda_i}{\sum_{i=1}^{15} \lambda_i}$ where λ_i are the means of the posterior distributions derived from MCMC simulation. From Table 7, it is clear that the AOGCMs are weighted differently during summer and winter, suggesting differential skills in reproducing present day climate.

Table 6. Model biases for 6 AOGCMs precipitation response to present climate (1961-1990) in London for winter and summer

Season	Model bias (%)					
	CGCM3T47	CGCM3T63	CSIROMK35	GISSAOM	MIROC32 HIRES	MIROC32 MEDRES
JJA	22.50	-2.12	6.50	12.07	-14.92	-14.10
DJF	2.18	-1.68	11.46	-0.04	-26.24	-5.64

Table 7. Relative weighting of the 15 AOGCM scenarios for 2050s of London for summer and winter seasons

Models/Scenarios	DJF	JJA
CGCMT47_A1B	2.22	4.07
CGCMT47_A2	1.11	1.09
CGCMT47_B1	7.76	2.80
CGCMT63_A1B	4.30	31.83
CGCMT63_A2	11.06	36.56
CGCMT63_B1	1.32	0.41
CSIROMK35_B1	2.46	1.10
CSIROMK35_A2	3.37	2.77
GISSAOM_A1B	18.21	2.66
GISSAOM_B1	24.25	4.10
MIROC32HIRES_A1B	0.07	4.28
MIROC32HIRES_B1	0.09	4.51
MIROC32MEDRES_A1B	8.75	1.26
MIROC32MEDRES_B1	8.44	0.69
MIROC32MEDRES_A2	6.57	1.86

4.1.3 Comparison of uncertainty estimation methods

This section presents a comparison of uncertainty estimation methods explained in sections 4.1.1 and 4.1.2 using density estimators. Fig. 5 and 6 present density estimates of mean precipitation change for winter and summer season with the results obtained from the WG combined kernel density estimates and the BA-REA method for London station using 2050s (2041-2070) time slice. The density estimate for the posterior distribution of the mean

precipitation change during summer using BA-REA method is under-smoothed, many spurious bumps especially at the tails for both winter and summer can be seen which makes it harder to understand the structure of the data. The estimates using kernel estimator show indication of smoothed structure. Also the kernel density estimator has indicated a wide range of precipitation change by the AOGCMs. Consideration of weights at every time step has enabled to identify the uncertainties among the AOGCMs.

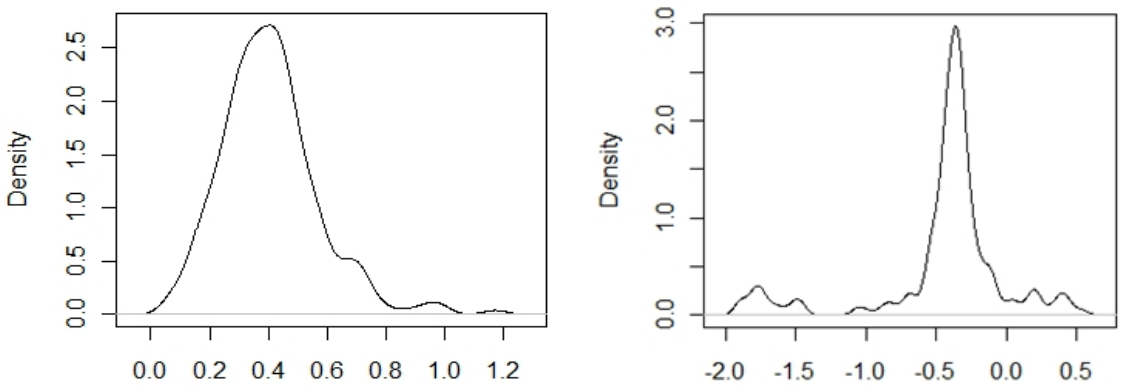

Fig. 5. Density estimate (y-axis) of the posterior distribution of mean precipitation change (x-axis) in London for (a) winter (DJF) [left] and (b) summer (JJA) [right] season using BA-REA method

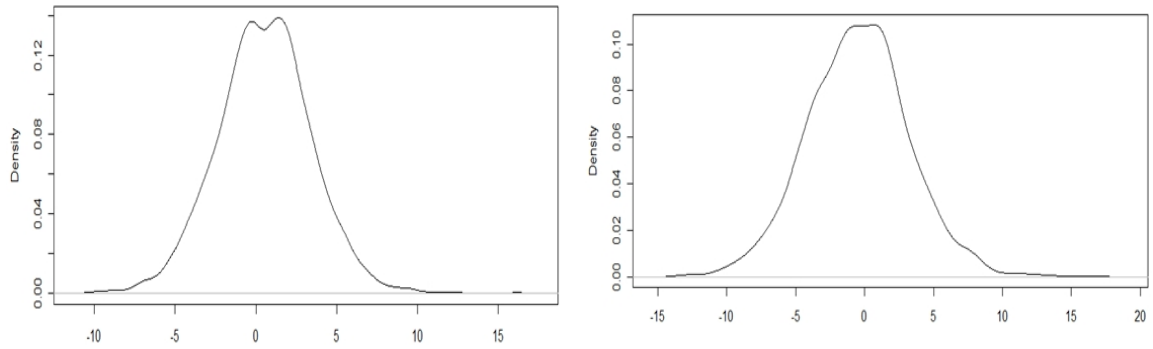

Fig. 6. Kernel density estimate (y-axis) of mean precipitation change (x-axis) in London for (a) winter (DJF) [left] and (b) summer (JJA) [right] season

The extended benefit of kernel estimators is that unlike BA-REA, the generated outputs can be modified into indices of interest and the probabilities can be calculated for any frequency of data, either monthly, or daily, or yearly, while the BA-REA method only provides the mean change combining the AOGCM scenarios. However, the kernel estimator has it's own limitations too. It cannot provide the explicit weight applicable to any data length, instead, the weight/kernel function (*K(.)*, in equation (2) can be calculated at specific points of interest within the range of data.

4.2 Uncertainty Estimation of Extreme Precipitation Events

4.2.1 Changes in future extreme precipitation events

Changes in the precipitation indices compared to the historic observed 1979-2005 values are computed from the downscaled precipitation for three time slices (2020s, 2050s, and 2080s) and presented in Table 8. Both summer and winter show different changing pattern. For summer, half of the scenarios show decrease in number of heavy precipitation and very wet days for 2020s and 2050s, but almost all models show increase in 5 day maximum precipitation amount, which clearly indicates higher intensity of precipitation during extreme precipitation events. For later part of the century (2080s), all three indices are showing increasing trend when compared to the 1979-2005 precipitation. However, for three time slices, range of changes are very high indicating higher uncertainties in model projections during summer. For winter, all but two cases are in agreement of the increasing trend of extreme precipitation indices for three time slices. In this case also, the uncertainty range is higher.

4.2.2 Kernel density estimators for quantifying uncertainties in extreme precipitation events

Selection of bandwidth: To measure how well the bandwidth selection methods perform, this section proceeds with the comparison of various bandwidth selectors by applying them in the assessment of extreme precipitation indices. Figs. 7 (a, b, c) presents kernel density estimates with statistics constructed using several bandwidth selectors: (i) the rule of thumb (ROT; by Silverman, 1986), (ii) likelihood cross validation (LCV) which searches for bandwidth based on likelihood (by Terrell and Hall, 1990) and (iii) the plug in estimator that selects the bandwidth using the pilot estimator of the derivatives refined by Sheather and Jones, 1991 (SJPI; named after Sheather-Jones plug in estimator). The choice of kernel is strictly limited to examining two most widely used types: Gaussian and Epanetchnikov kernels. The 'original' estimate is created by mixing the inputs and 1000 samples are generated from the mixtures without any estimation of bandwidth. It is created for assessing how different techniques respond to the original data type. Comparing the generated estimators it is seen that the density estimate using ROT is highly oversmoothed which may have missed important features of the generated data. For both kernel types, it failed to capture the multimodality. In case of LCVs, there are suggestions of multiple modes in the density curve. But it is still severely undersmoothed; the small bumps occurring from the uncertainties of different AOGCM types makes it harder to understand the structure of real data. The bandwidth by SJPI seems to be in a better agreement with the 'original' estimate and provides a strong indication of multimodal distribution. From Figs. 7(a), 7(b) and 7(c), it is also evident that the choice of kernel merely plays a role in estimation of density. So for the present study, the Gaussian kernel with Sheather-Jones plug in estimator was used to calculate the bandwidth for estimating density of the extreme precipitation indices.

Uncertainty estimation: To examine uncertainties in future extreme precipitation events, the yearly values of the indices from each AOGCMs and scenarios are taken as a set of independent realizations. This set is then used at each time step to establish a PDF by applying the bandwidth values in equation 2. The CDF values at the upper and lower ranges of each severity class are calculated by numerical integration. The difference between the upper and lower value can thus be considered as the probability of that specific class of extreme precipitation indices for future. Figs. 8 and 9 present the probability of heavy precipitation days and 5 day precipitation for 2020s, 2050s and 2080s.

Table 8. Percent changes in extreme precipitation events for 2020s, 2050s and 2080s as compared to 1979-2005

Models/Scenarios	Heavy precipitation days			Very wet days			5 day precipitation		
	2020s	2050s	2080s	2020s	2050s	2080s	2020s	2050s	2080s
Summer									
CGCM3T47_A1B	1.38	-7.70	4.09	3.30	15.68	3.68	-0.23	12.73	3.05
CGCM3T47_A2	0.00	-11.32	0.00	0.00	13.21	0.00	0.00	14.08	0.00
CGCM3T47_B1	6.01	-5.21	2.52	9.14	9.83	9.05	2.26	15.29	3.02
CGCM3T63_A1B	2.79	-8.43	9.22	12.44	18.28	17.26	14.73	18.11	10.17
CGCM3T63_A2	-5.97	-9.20	9.35	-7.19	13.66	14.63	-2.55	24.61	14.62
CGCM3T63_B1	-2.99	0.97	2.19	-0.10	34.16	5.79	-0.57	29.30	3.79
CSIROMK3.5_A2	10.77	3.78	25.68	23.62	37.76	48.00	12.54	36.90	27.56
CSIROMK3.5_B1	-1.02	15.19	13.07	-2.24	63.22	22.21	-2.68	44.39	11.77
GISSAOM_A1B	5.46	3.97	27.50	8.94	38.44	51.79	5.08	31.63	29.69
GISSAOM_B1	9.74	2.94	20.39	17.40	40.02	38.00	10.27	31.15	25.79
MIROC3HIRES_A1B	-12.89	-17.72	-8.64	-17.59	-7.18	-17.05	-8.35	3.64	-11.52
MIROC3HIRES_B1	-1.34	-19.51	2.44	1.65	-3.69	3.37	0.48	8.73	1.82
MIROC3MEDRES_A1B	-3.22	-19.84	-19.02	-3.01	-7.07	-26.74	-4.17	2.73	-16.10
MIROC3MEDRES_A2	-3.10	-16.29	-28.91	-2.82	1.38	-43.89	-6.27	6.43	-29.08
MIROC3MEDRES_B1	-5.19	-9.20	-0.50	-4.86	13.99	-0.32	-2.15	17.29	0.29
Winter									
CGCM3T47_A1B	25.24	35.25	45.20	84.00	107.98	123.88	27.07	38.78	40.94
CGCM3T47_A2	28.33	44.52	56.42	85.42	126.02	147.86	30.96	42.01	53.00
CGCM3T47_B1	22.25	28.64	40.85	76.16	87.56	114.62	29.29	32.18	34.69
CGCM3T63_A1B	30.27	31.37	44.05	82.10	84.71	126.97	27.40	29.32	42.39
CGCM3T63_A2	19.68	14.23	42.48	66.90	53.85	117.95	26.56	19.76	40.08
CGCM3T63_B1	**30.85**	**34.41**	**27.49**	**72.84**	**106.79**	**88.75**	**28.17**	**35.73**	**28.75**
CSIROMK3.5_A2	11.67	26.23	25.03	40.55	87.80	85.90	12.09	28.13	30.39
CSIROMK3.5_B1	**7.95**	**18.90**	**6.37**	**41.50**	**56.70**	**34.38**	**12.50**	**27.36**	**14.65**
GISSAOM_A1B	14.60	16.33	34.46	55.03	47.44	102.75	**20.86**	**15.05**	**35.36**
GISSAOM_B1	25.66	17.85	25.34	72.60	68.57	77.11	28.57	22.46	23.10
MIROC3HIRES_A1B	18.64	30.32	28.07	59.78	87.56	93.73	27.94	32.09	28.20
MIROC3HIRES_B1	19.63	18.27	42.06	49.57	68.33	106.79	18.82	24.32	37.83
MIROC3MEDRES_A1B	9.26	15.33	15.44	41.74	51.00	62.16	10.93	15.49	26.34
MIROC3MEDRES_A2	9.73	12.61	21.05	50.52	48.15	77.59	12.50	13.12	24.33
MIROC3MEDRES_B1	6.95	13.34	22.51	39.60	51.95	65.48	15.89	18.58	21.46

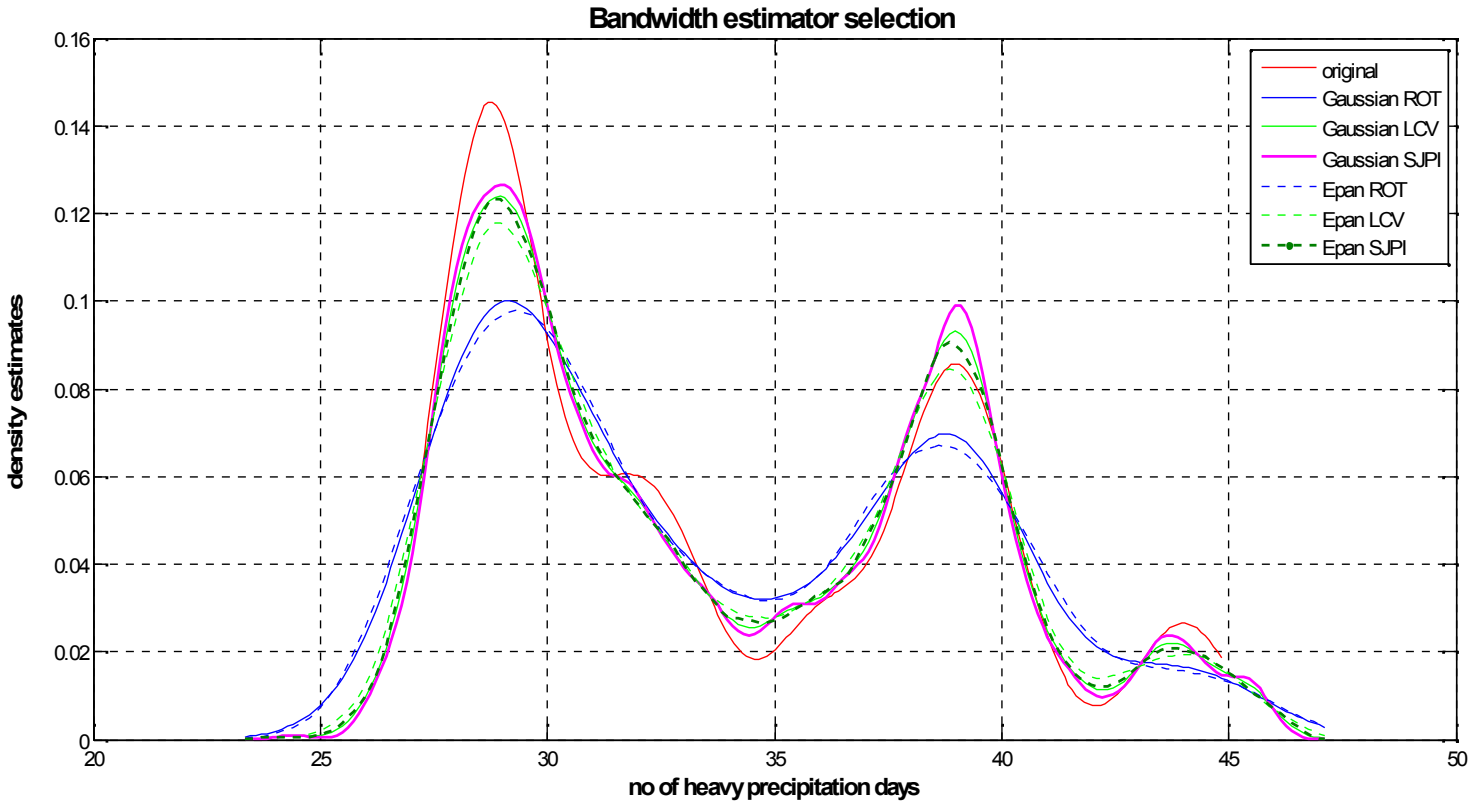

Fig. 7(a). Gaussian and Epanetchnikov kernel estimates of heavy precipitation days using various data-driven bandwidths: rule of thumb (ROT; by Silverman '86), least square cross validation (LCV), plug-in type estimator (SJPI; Sheather-Jones '91)

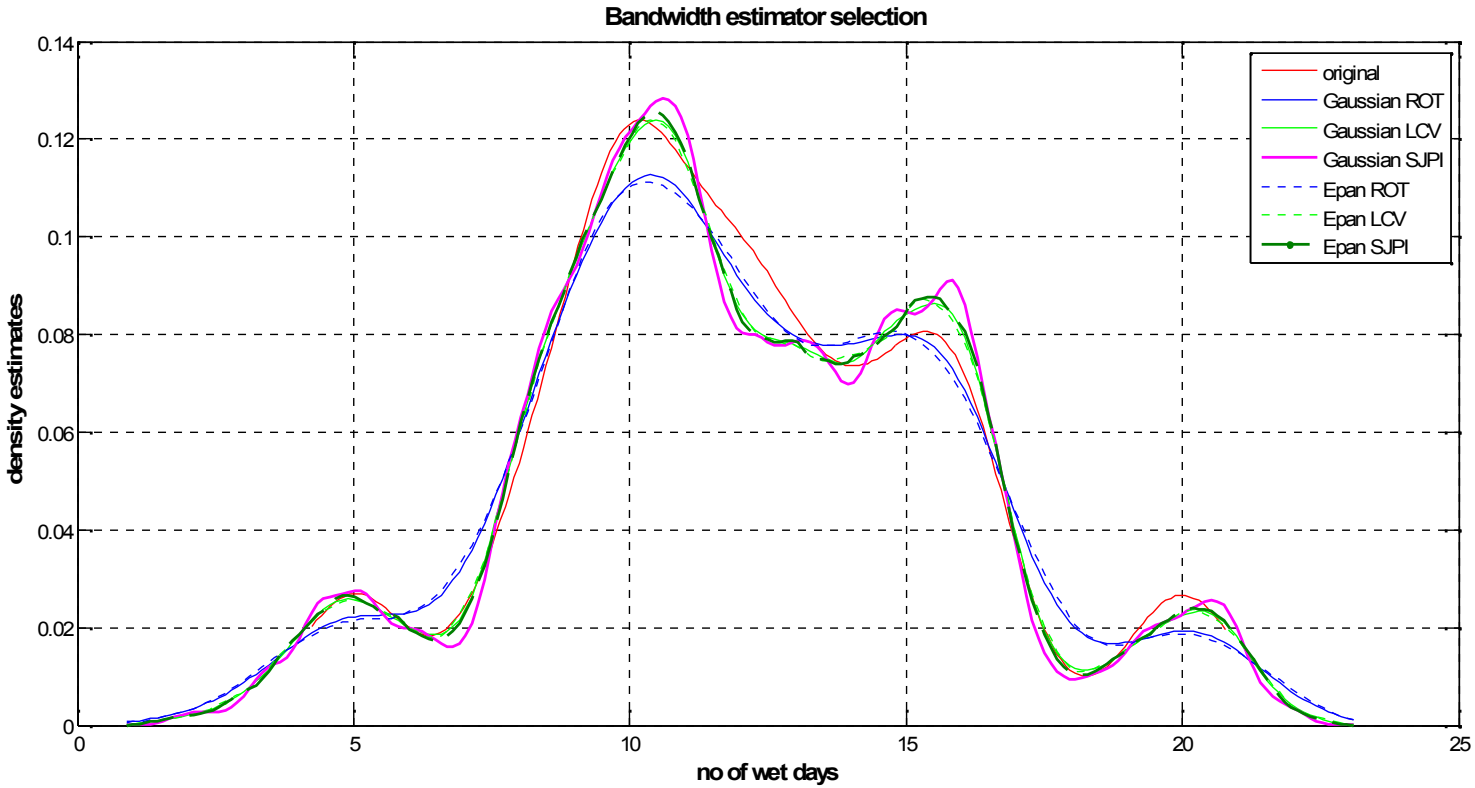

Fig. 7(b). Gaussian and Epanetchnikov kernel estimates of very wet days using various data-driven bandwidths: rule of thumb (ROT; by Silverman '86), least square cross validation (LCV), plug-in type estimator (SJPI; Sheather-Jones '91)

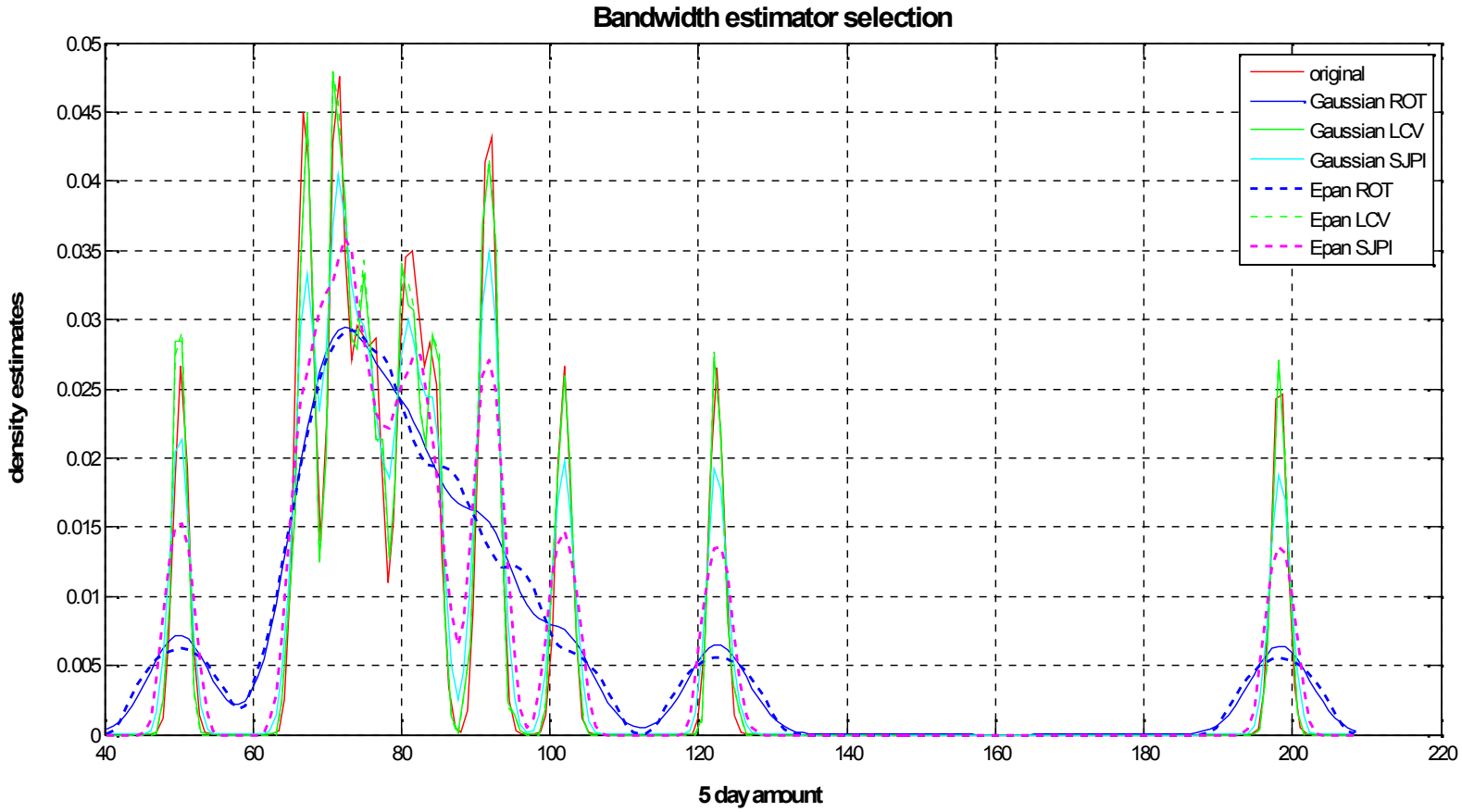

Fig. 7(c). Gaussian and Epanetchnikov kernel estimates of 5 day precipitation using various data-driven bandwidths: rule of thumb (ROT; by Silverman '86), least square cross validation (LCV), plug-in type estimator (SJPI; Sheather-Jones '91)

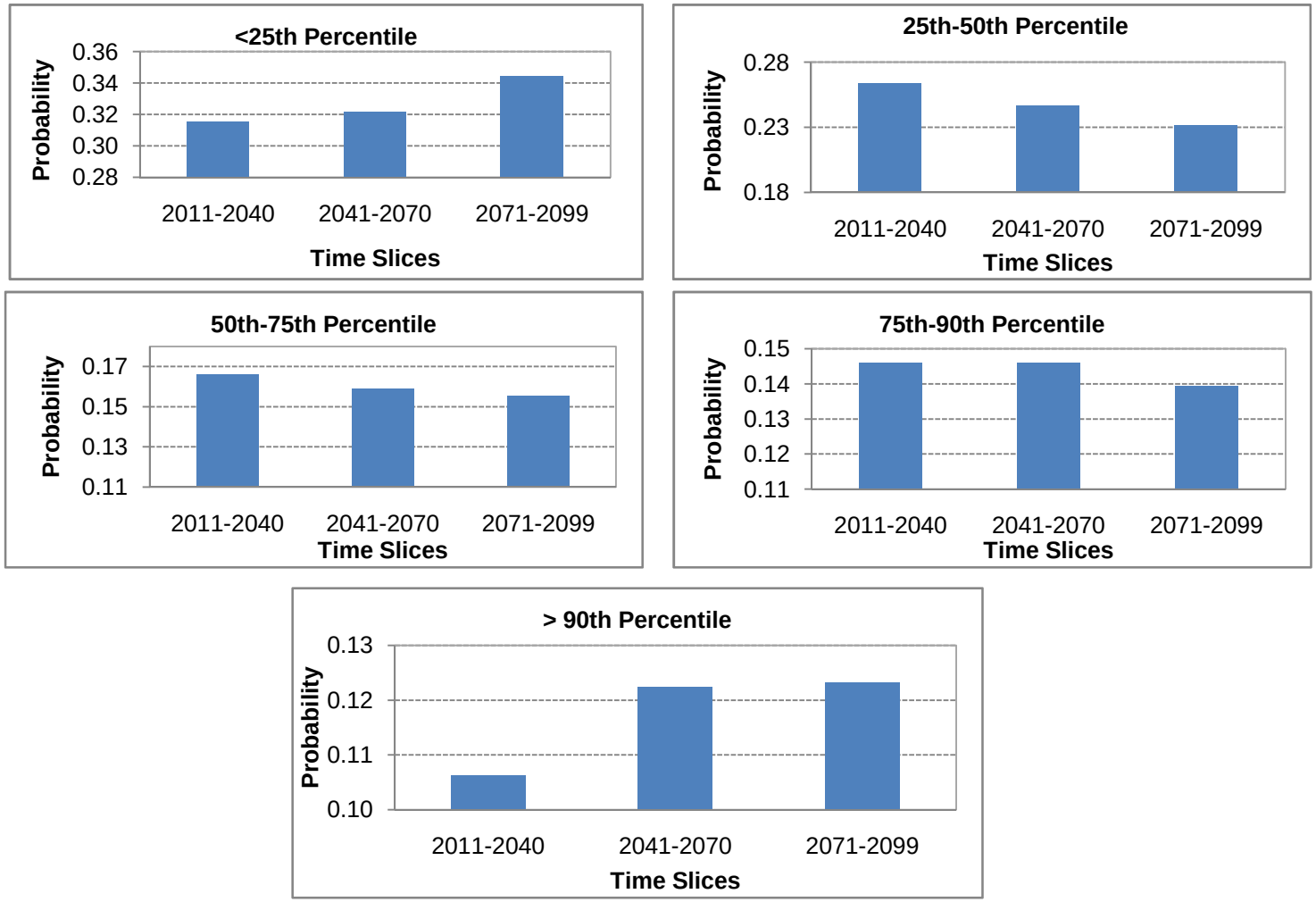

Fig. 8(a). Probability of heavy precipitation days during summer using kernel density estimation

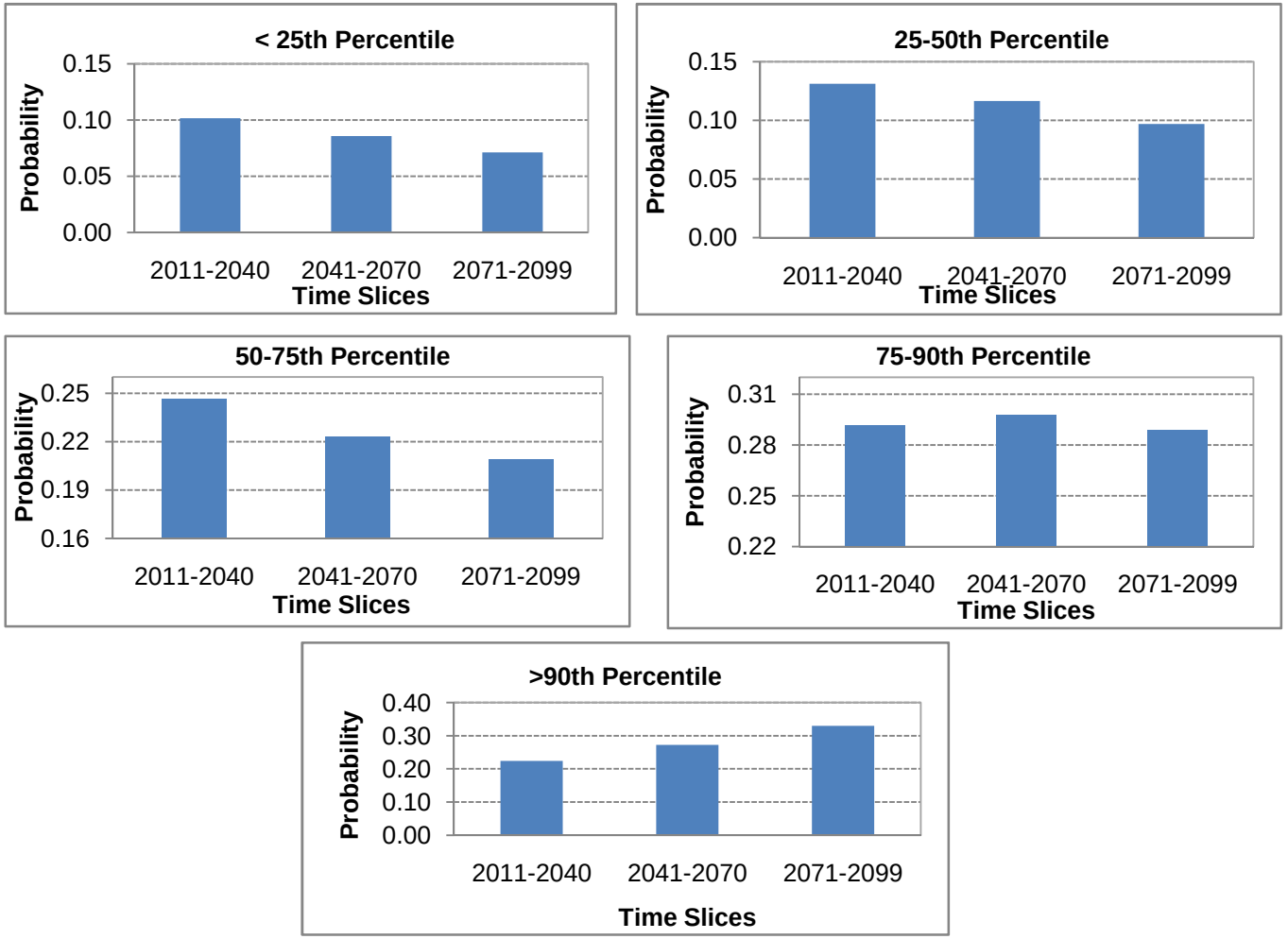

Fig. 8(b). Probability of heavy precipitation days during winter using kernel density estimation

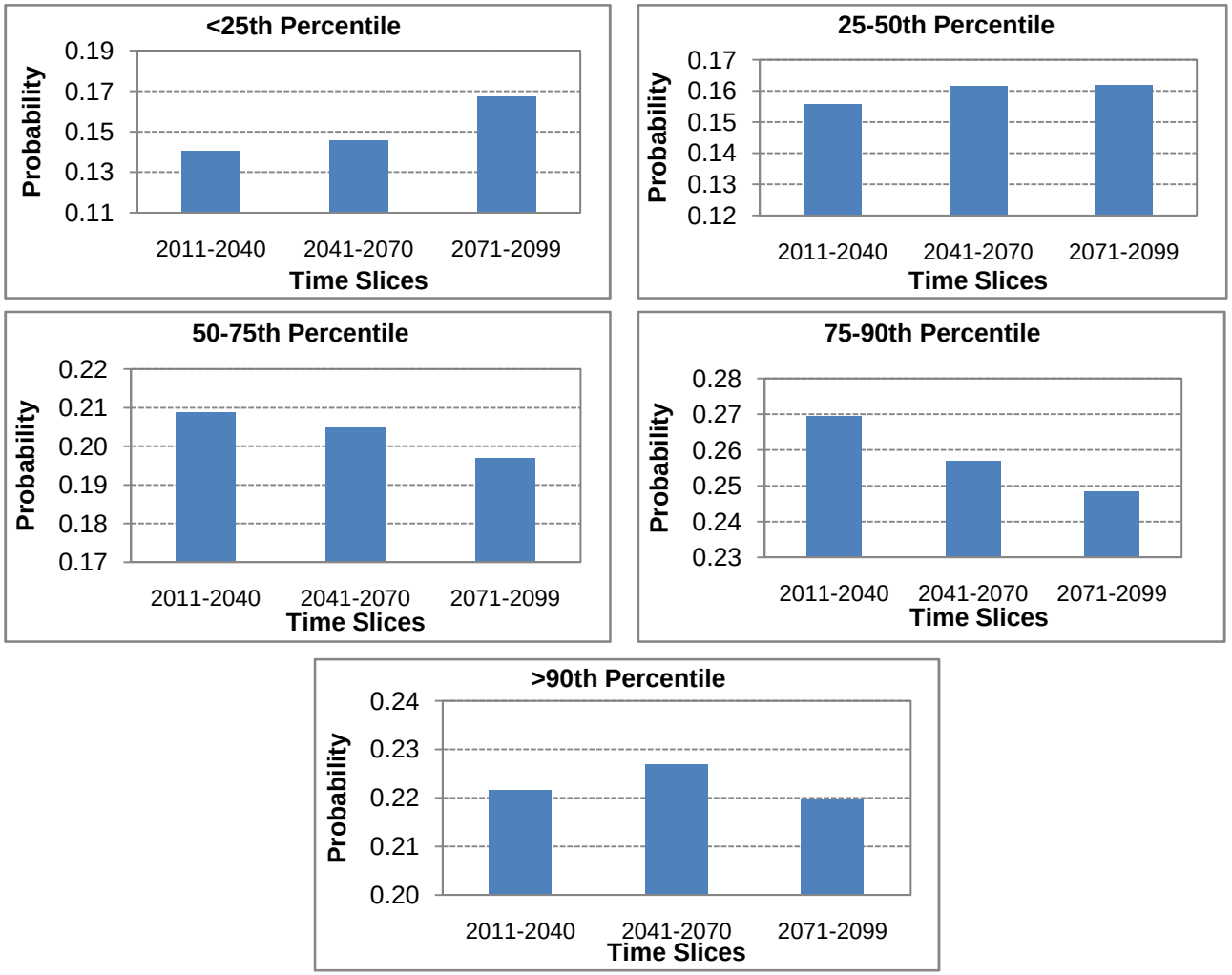

Fig. 9(a). Probability of 5 day precipitation during summer using kernel density estimation

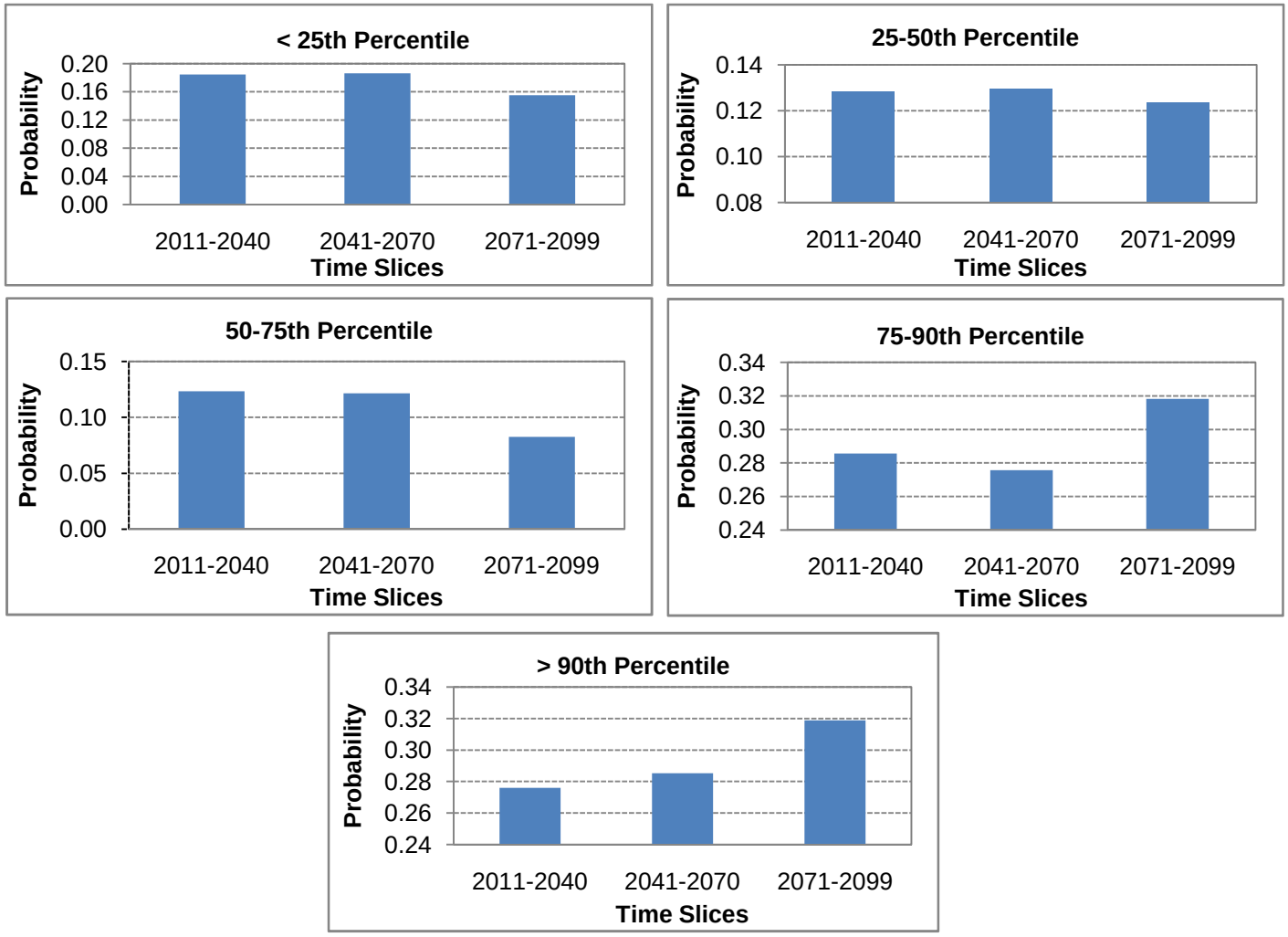

Fig. 9(b). Probability of 5 day precipitation during winter using kernel density estimation

Both indices show somewhat similar results for summer and winter season, with winter projecting more clearly visible trend than summer. For heavy precipitation days, the near normal condition shows slight increase in probabilities for later part of the century. For mild and moderate conditions, probabilities decrease slightly while approaching 2100. Probabilities for the extreme condition increase over the time slices indicating the increase in higher number of heavy precipitation days over the later part of the century. This trend is supported by the probabilities of 5 day precipitation for summer. Severe and extreme cases show increasing probabilities or the increase in intensity of precipitations over summer season.

For the winter season, a different pattern is visible. Near normal, mild and moderate cases show decreasing probabilities for both heavy precipitation days and 5 day precipitation. For severe and extreme conditions, probability increases when approaching 2100, indicating increase in both frequency and intensity of higher end extreme precipitation level.

The methods explained can be seen as a major improvement over the 'normal' kernel (Silverman, 1986) method applied in other AOGCM and scenario uncertainty studies. The SJPI based kernel estimation method proposed here overcomes the limitations of assumptions of normality in case of unknown densities/distributions. It is completely data driven; hence, more robust, flexible, and independent and the methodology has been extensively revised by statisticians.

The Orthomornal method (Efromovich, 1999) proposed by Ghosh and Mujumder (2007) to estimate uncertainties of future droughts provides another important segment of nonparametric uncertainty estimation technique. However, one major limitation of orthonormal method is the use of a subset of Fourier series consisting of cosine functions without proper justification. The additional benefit of kernel density estimators for estimating AOGCM and scenario uncertainties appears from the fact that the scientific community is now highly confident that the trends in precipitation over future period are not going to follow the same distribution as in the past. However, it is true for any statistical method that larger sample provides better estimates of any data distribution. It is our expectation that with the advance of more sophisticated global climate models, kernel method will be applied with more confidence for uncertainty estimation problems.

5. CONCLUSIONS

This study deals with the approaches for quantifying AOGCM and scenario uncertainties from the modeled outputs of extreme precipitation events for London, Ontario, Canada. This work is strictly limited to the uncertainties of the outputs from several AOGCMs and scenarios and does not consider the uncertainties due to parameterization or structure of the models.

A comparison between BA-REA method and kernel density estimates of downscaled AOGCM outputs revealed that while the BA-REA method can be a good alternative for predicting mean changes in precipitation in any region, it cannot be used in estimation of uncertainties of different extreme events occurring on a daily time scale. Furthermore, the choice of analyzing outputs is fairly limited in BA-REA methods. The capability of the BA-REA method to analyze the climate responses is fairly limited; whereas, the downscaled outputs can be modified into any indices of interest and kernel estimators can be used to calculate probabilities of any frequency of data, monthly or daily or yearly time scale by accounting associated uncertainties, instead of calculating equal weights based on the

means. It has a significant implication for estimating uncertainties of extreme precipitation events; calculating weights based on the mean can ignore the higher or lower values which may cause an unrealistic representation of climate extremes, such as floods, droughts, etc. However, the kernel estimator has its limitations too, from the extended chance of over or under-smoothing resulting from wrong selection of bandwidth. The comparison of the best fit curves for different AOGCM scenarios for extreme precipitation indices shows varying agreement and thereby the limited benefits of parametric distribution approach.

The choice of an appropriate bandwidth selection method is a significant step for kernel estimation. The shape of the distribution function is important in determining the performance of the bandwidth. The comparative results of different bandwidth selectors show that the rule of thumb (ROT) method assuming normal kernel suffers from over-smoothing for both indices while the least square cross validation (LCV) method results in under-smoothed distributions. The Sheather Jones plug in (SJPI) estimator offered a useful compromise between the ROT and the LCV methods. This trade-off between the distributions of the bandwidths seems to be an intrinsic criterion for assessing the performance of data-driven bandwidth selectors. Using the SJPI bandwidths, the CDFs for different severity classes are calculated for the extreme precipitation indices. The analyses are based on the assumption that the outputs from different AOGCMs are independent realizations; hence, indices have a different PDF at each time step and are not limited to any specific type of distribution.

Overall, the comparison between two different multi-model uncertainty ensemble models has provided useful information. The variable weight method combining downscaling based on a principal component integrated weather generator and data driven kernel density estimator is capable of considering the AOGCM outputs as individual realization at each time step, rather than depending on their performances based on the mean or bias values. The prevalent conception of the increased intensity of extreme precipitation indices resulting from climate change are quantified with probability information. Classifying these indices based on their severity level has added useful insight to the occurrence of those extreme rare events (events with >75th percentile values). The nonparametric methods, hence, can be seen as a major improvement over the parametric methods which assume specific distributions for estimating uncertainties. Considering the probabilities obtained, it can be said that the probability of severe and extreme events are going to increase for both summer and winter due to the changes in climate over next century.

Future scope of the study includes generating probabilistic intensity-duration-frequency (IDF) curves for future extreme precipitation events by incorporating associated uncertainties from AOGCM and scenario outputs for decision making.

ACKNOWLEDGEMENT

The authors wish to gratefully thank Canadian Foundation for Climate and Atmospheric Sciences for providing financial assistance. The constructive comments by Dr. Claudia Tebaldi of National Centre of Atmospheric Research for improving the BA-REA methodology are greatly acknowledged. Finally, the authors would like to thank Ms. Leanna King for helping in database generation and organization process.

COMPETING INTERESTS

Authors have declared that no competing interests exist.

REFERENCES

Adamowski, K. (1985). Nonparametric kernel estimation of flood frequencies. Water Resources Research, 21(11), 1585-1590.

Allan, M.R., Ingram, W.J. (2002). Constraints on future changes in climate and the hydrologic cycle. Nature, 419, 224– 232.

Allan, M.R., Stott, P.A, Mitchell, J.F.B., Schnur, R., Delworth, T.L. (2000). Quantifying the uncertainty in forecasts of anthropogenic climate change. Nature, 407, 617– 620.

Bardossy, A. (1997). Downscaling from GCM to local climate through stochastic linkages. Journal of Environmental Management, 49, 7-17.

Benestad, R.E. (2004). Tentative probabilistic temperature scenarios for northern Europe. Tellus, Ser. A, 56, 89–101.

Bowman, A.W. (1984). An Alternative Method of Cross-Validation for the Smoothing of density estimates. Biometrika, 71, 353-360.

Brown, M.B., Forsythe, A.B. (1974). Robust tests for the equality of variances. Journal of the American Statistical Association, 69, 364-367.

Buytaert, W., Ce´lleri, R., Timbe, R. (2009). Predicting climate change impacts on water resources in the tropical Andes: Effects of GCM uncertainty. Geophysical Research Letters, 36, L07406, doi:10.1029/2008GL037048.

Castro, C.L., Pielke, Sr., R.A., Adegoke, J.O. (2007). Investigation of the summer climate of the contiguous United States and Mexico using the regional atmospheric modeling system (RAMS). Part I: Model Climatology (1950-2002). Journal of Climate, 20, 3844–3864.

Choi, W., Moore, A., Rasmussen, P.F. (2007). Evaluation of temperature and precipitation data from NCEP-NCAR Global and Regional Reanalyses for hydrological modeling in Manitoba. In Proceedings of the CSCE 18th Hydrotechnical Conference on Challenges for Water Resources Engineering in a Changing World. Winnipeg, Manitoba., 1-10.

Choi, W., Jim, S.T., Rasmussen, P.F., Moore, A.R. (2009). Use of the North American regional reanalysis for hydrologic modelling in Manitoba. Canadian Water Resources Journal, 34(1), 17-36.

Cubasch, U., Meehl, G.A., Boer, G.J., Stouffer, R.J., Dix, M., Noda, A., Senior, C.A., Raper, S., Yap, K.S. (2001). The scientific basic. Contribution of working group 1 to the third assessment report of the intergovernmental panel of climate change. Cambridge University Press, Cambridge, UK and New York, USA, 881.

Ensor, L.A., Robeson, S.M. (2008). Statistical characteristics of daily precipitation: comparisons of gridded and point datasets. Journal of Applied Meteorology and Climatology, 47(9), 2468- 2476.

Furrer, E.M, Katz, R.W. (2008). Improving the simulation of extreme precipitation events by stochastic weather generators. Water Resources Research, 44, W12439, doi: 10.1029/2008WR007316.

Ghosh, S., Majumdar, P.P. (2007). Nonparametric methods for modeling GCM and scenario uncertainty in drought assessment. Water Resources Research, 43, W07495, 19, doi:10.1029/2006WR005351.

Giorgi, F., Mearns, L.O. (2003). Probability of regional climate change calculated using the reliability ensemble averaging (REA) method. Geophysical Research Letters, 30(12), 1629, doi: 10.1029/2003GL017130.

Haberlandt, U., Kite, G.W. (1998). Estimation of daily space-time precipitation series for macroscale hydrologic modeling. Hydrological Processes, 12, 1419-1432.

Hall, P., Marron, J.S. (1991). Lower bounds for bandwidth selection in density estimation. Probability Theory and Related Fields, 90, 149-173.

Hennessy, K.J., Mitchell, J.F.B. (1997). Changes in daily precipitation under enhanced greenhouse conditions. Climate Dynamics, 13, 667-680.

Hughes J.P. (1993). A class of stochastic models for relating synoptic atmospheric patterns to local hydrologic phenomena. Ph.D. thesis, University of Washington, US.

Hughes J.P., Guttorp, P., Charles, S.P. (1999). A non-homogeneous hidden markov model for precipitation occurrence. Appl. Statist., 48(1), 15-30.

Hughes, J.P., Guttorp, P. (1994). A class of stochastic models for relating synoptic atmospheric patterns to regional hydrologic phenomena. Water Resources Research, 30(5), 1535–1546.

Intergovernmental Panel on Climate Change (IPCC). (2007). Climate Change 2007: Impacts, adaptation and vulnerability. Contribution of working Group II to the Fourth Assessment Report of the Intergovernmental Panel on Climate Change, edited by M. Parry et al., Cambridge University Press, UK.

IPCC. (2007). Climate Change 2007: The Physical Science Basis. Contribution of working group 1 to the Fourth Assessment Report of the Intergovernmental Panel of Climate Change, Annexes [Baede, A.P.M. (ed.)]. Cambridge University Press, Cambridge UK and New York, USA, 48.

Jackson, C., Sen, M.K., Stoffa, P.L. (2004). An efficient stochastic Bayesian approach to optimal parameter and uncertainty estimation for climate model predictions. J. Climate, 17, 2828–2841.

Jones, M.C., Marron, J.S., Sheather, S.J. (1996). A brief survey of bandwidth selection for density estimation. Journal of the American Statistical Association, 91(433), 401–407.

Kalnay, E., Kanamitsu, M., Kistler, R., Collins, W., Deaven, D., Gandin, L., Iredell, M., Saha, S., White, G., Woolen, J., Zhu, J., Chelliah, M., Ebisuzaki, W., Higgins, W., Janowiak, J., Mo, C., Ropelewski, C., Wang, J., Leetmaa, A., Reynolds, R., Jenne, R., Joseph, D. (1996). The NCEP-NCAR Reanalysis Project. Bulletin of the American Meteorological Society, 77(3), 437–471.

Kilsby C.G., Jones, P.D., Burton, A., Ford, A.C., Fowler, H.J., Harpham, C., James, P., Smith, A., Wilby, R.L. (2007). A daily weather generator for use in climate change studies. Environmental Modelling and Software*, 22,* 1705-1719.

Koutsoyiannis D. (2004). Statistics of extremes and estimation of extreme rainfall, 1, Theoretical investigation, Hydrological Sciences Journal, 49 (4), 575–590.

Lall, U. (1995). Nonparametric function estimation: recent hydrologic contributions. Reviews of Geophysics, Contributions in Hydrology, U.S. National Report to the IUGG 1991-1994, 1093-1099.

Lall, U., Rajagopalan, B., Tarboton, D.G. (1996). A nonparametric wet/dry spell model for daily precipitation. Water Resources Research, 32(9), 2803-2823.

Levene, H. (1980). Contributions to probability and statistics. Stanford University Press, USA.

Loader, C. (1999). Classical or Plug-In?, The Annals of Statistics, 27(2), 415-438.

Marron, J.S., Wand, M.S. (1992). Exact mean integrated squared error. Annals of Statistics, 20, 712-736.

Mailhot, A., Kingumbi, A., Talbot, G., Poulin, A. (2010). Future changes in intensity and seasonal pattern of ocurrences of daily and multi-day annual maximum precipitation over Canada. J. Hydrol., 388(3-4), 173-185.

Mailhot, A., Beauregard, I., Talbot, G., Caya, D., Biner, S. (2011). Future changes in intense precipitation over Canada assessed from multi-model NARCCAP ensemble simulations. Int. J. Climatol., DOI: 10.1002/joc.2343.

Mailhot, A., Duchesne, S., Caya, D., Talbot, G. (2007). Assessment of future change in intensity-duration-frequency (IDF) curves for Southern Quebec using the Canadian Regional Climate Model (CRCM). J. Hydrol., 347(1-2), 197-210.

Mesinger, F., DiMego, G., Kalnay, E., Mitchell, K., Shafran, P.C., Ebisuzaki, W., Jovic, D., Wollen, J., Rogers, E., Berbery, E.H., Ek, M.B, Fan, Y., Grumbine, Y., Higgins, W., Ki, H., Lin, Y., Mankin, H., Parrish, D., Shi, W. (2006). North American Regional Reanalysis, Bulletin of the American Meteorological Society, 87(3), 343-360.

New, M., Hulme, M. (2000). Representing uncertainty in climate change scenarios: a Monte-Carlo approach. Integrated Assessment, 1, 203-213.

Nigam, S., Ruiz-Barradas, A. (2006). Seasonal hydroclimate variability over North American Global and Regional Reanalyses and AMIP simulations: varied representation. Journal of Climate, 19(5), 815-837.

Polansky, A.M., Baker, E.R. (2000). Multistage plug-in bandwidth selection for kernel distribution function estimates. Journal of Statistical Computation and Simulation, 65, 63-80.

Prodanovic, P., Simonovic, S.P. (2006). Inverse flood risk modelling of The Upper Thames River Watershed. Water Resources Research Report no. 052, Facility for Intelligent Decision Support, Department of Civil and Environmental Engineering, London, Ontario, Canada, 163 pages. ISBN: (print) 978-0-7714-2634-6; (online) 978-0-7714-2635-3.

Prudhomme, C., Jakob, D., Svensson, C. (2003). Uncertainty and climate change impact on the flood regime of small UK catchments. Journal of Hydrology, 277, 1–23.

Raisanen, J., Palmer, T.N. (2001). A probability and decision-model analysis of a multimodel ensemble of climate change simulations. J. Climate, 14, 3212– 3226.

Randall, D.A., Wood, R.A., Bony, S., Colman, R., Fichefet, T., Fyfe, J., Kattsov, V., Pitman, A., Shukla, J., Srinivasan, J., Stouffer, R.J., Sumi, A., Taylor, K.E. (2007). Climate Models and Their Evaluation. In: Climate Change 2007: The Physical Science Basis. Contribution of Working Group I to the Fourth Assessment Report of the Intergovernmental Panel on Climate Change [Solomon, S., D. Qin, M. Manning, Z. Chen, M. Marquis, K.B. Averyt, M. Tignor and H.L. Miller (eds.)]. Cambridge University Press, Cambridge, United Kingdom and New York, NY, USA.

Reid, P.A., Jones, P.D., Brown, O., Goodess, C.M., Davies, T.D. (2001). Assessments of the reliability of NCEP circulation data and relationships with surface climate by direct comparisons with station based data. Climate Research, 17, 247–261.

Robeson, S.M., Ensor, L.A. (2006). Comments on “Daily precipitation grids for South America”. Bulletin of American Meteorological Society, 87, 1095-1096.

Rudemo, M. (1982). Empirical choice of histograms and kernel density estimators. Scandinavian Journal of Statistics, 9, 65-78.

Rusticucci, M.M., Kousky, V.E. (2002). A comparative study of maximum and minimum temperatures over Argentina: NCEP-NCAR Reanalysis versus station data. Journal of Climate, 15(15), 2089-2101.

Salathe Jr., E.P. (2003). Comparison of various precipitation downscaling methods for the simulation of streamflow in a rainshadow river basin. International Journal of Climatology, 23, 887-901.

Scott, D.W., Terrell, G.R. (1987). Biased and unbiased cross- validation in density estimation. Journal of the American Statistical Association, 82, 1131-1146.

Semenov, M.A., Barrow, E.M. (1997). Use of a stochastic weather generator in the development of climate change scenarios. Climatic Change, 35, 397-414.

Sharif, M., Burn, D.H. (2006). Simulating climate change scenarios using an improved K-nearest neighbor model. Journal of Hydrology, 325, 179-196.

Sharma, A., Tarbaton, D.G., Lall, U. (1997). Streamflow simulation – a nonparametric approach. Water Resources Research, 33(2), 291-308.

Sheather, S.J. (1983). A data-based algorithm for choosing the window width when estimating the density at a point. Computational Statistics and Data Analysis, 1, 229-238.

Sheather, S.J. (1986). An improved data-based algorithm for choosing the window width when estimating the density at a point. Computational Statistics and Data Analysis, 4, 61-65.

Sheather, S.J., Jones, M.C. (1991). A reliable data-based bandwidth selection method for kernel density estimation. Journal of the Royal Statistical Society, Ser. B, 53, 683-690.

Silverman, B.W. (1986). Density estimation for statistics and data analysis. Monographs on Statistics and Applied Probability, Chapman & Hall/ CRC., Washington, D.C.

Smith, R.L., Tebaldi, C., Nychka, D., Mearns, L. (2009). Bayesian modeling of uncertainty in ensembles of climate models. Journal of the American Statistical Association, 104 (485), 97-116., doi:10.1198/jasa.2009.0007.

Solaiman, T.A., Simonovic, S.P. (2010). National centers for environmental predicton - national center for atmospheric research (NCEP-NCAR) reanalyses data for hydrologic modelling on a basin scale. Canadian Journal of Civil Engineering, 37(4), 611-623.

Solaiman, T.A., King, L.M., Simonovic, S.P. (2011). Extreme precipitation vulnerability in the Upper Thames river basin: uncertainty in climate model projections. International Journal of Climatology, 31(5), 2350-2364.

Stainforth, D.A., Downing, T.E. Lopez, R.W.A., New, M. (2007). Issues in the interpretation of climate model ensembles to inform decisions. Philos. Trans. R. Soc., Ser. A, 365, 2163–2177.

Stone, D.A., Allan, M.R. (2005). The end-to-end attribution problem: From emissions to impacts. Climate. Change, 77, 303– 318.

Sun, Y., Solomon, S., Dai, A., Portman, R. (2006). How often does it rain?, Journal of Climate, 19, 916–934.

Tebaldi, C., Mearns, L.O., Nychka, D., Smith, R.L. (2004). Regional probabilities of precipitation change: A Bayesian analysis of multimodel simulations. Geophysical Research Letters, 31.

Tebaldi, C., Smith, R.L., Nychka, D., Mearns, L.O. (2005). Quantifying uncertainty in projections of regional climate change: a bayesian approach to the analysis of multimodel ensembles. Journal of Climate, 18(10), 1524-1540.

Tebaldi, C., Smith, R.L. (2010). Characterizing uncertainty of climate change projections using hierarchical models. In The Oxford Handbook of Applied Bayesian Analysis [eds. O'Hagan, T. and West, M.], Oxford University Press, UK, 896.

Terrell, G.R. (1990). The maximal smoothing principle in density estimation. Journal of the American Statistical Association, 85, 470-477.

Terrell, G.R., Scott, D.W. (1985). Oversmoothed nonparametric density estimates. Journal of the American Statistical Association, 80, 209-214.

Tolika, K., Maheras, P., Flocas, H.A., Imitriou, A-P. (2006). An evaluation of a general circulation model (GCM) and the NCEP-NCAR reanalysis data for winter precipitation in Greece. International Journal of Climatology, 26, 935–955.

Vincent, L.A., Mekis, E. (2006). Changes in daily and extreme temperature and precipitation indices for Canada over the twentieth century. Atmosphere-Ocean, 44(2), 177-193.

Wilby, R.L., Harris, I. (2006). A framework for assessing uncertainties in climate change impacts: Low-flow scenarios for the River Thames, UK. Water Resources Research, 42, W02419, doi: 10.1029/2005WR004065.

Wilby, R.L., Wigley, T.M.L. (2000). Precipitation predictors for downscaling: observed and general circulation model relationships. International Journal of Climatology, 20, 641-661.

Wilks D.S., Wilby, R.L. (1999). The weather generation game: a review of stochastic weather models. Progress in Physical Geography, 23(3), 329-357.

Woo, M-K., Thorne, R. (2006). Snowmelt contribution to discharge from a large mountainous catchment in subarctic Canada. Hydrologic Processes, 20, 2129-2139.

Yates D., Gangopadhyay, S., Rajagopalan, B., Strzepek, K. (2003). A technique for generating regional climate scenarios using a nearest-neighbour algorithm. Water Resources Research, 39(7), 1199-1213.

Zhang, X., Vincent, L.A., Hogg, W.D., Niitsoo, A. (2000). Temperature and precipitation trends in Canada during the 20th century. Atmosphere-Ocean, 38, 395-429.